

METHODOLOGICAL NOTES

PACS numbers: **52.35.–g**, **52.65.–y**

One-dimensional modulational instability models of intense Langmuir plasma oscillations using the Silin–Zakharov equations

A G Zagorodny, A V Kirichok, V M Kuklin

DOI: 10.3367/UFNe.2016.01.037697

Contents

Abstract. **The modulational instability mechanisms of intense Langmuir oscillations in a plasma are reviewed both for field energy densities below (Zakharov's model) and above (Silin's model) the plasma's thermal energy density. It is shown by a one-dimensional example that V E Zakharov's mechanism involving nonlinear absorption of Langmuir oscillations in plasma also holds for intense cold plasma fields described by V P Silin's model. It is also shown that the development mechanisms of the modulational instability of Langmuir oscillations are similar for nonisothermal and cold plasmas. Hybrid models treating electrons quasihydrodynamically and ions as particles are analyzed in detail, which allows the study of the direct mechanism by which energy is transferred to ions in the instability development process.**

A G Zagorodny Bogolyubov Institute for Theoretical Physics,
14-b Metrolohichna str., 03680 Kiev, Ukraine
E-mail: Zagorodny@nas.gov.ua
A V Kirichok Bogolyubov Institute for Theoretical Physics,
14-b Metrolohichna str., 03680 Kiev, Ukraine;
V N Karazin Kharkiv National University,
4 Svobody sq., 61022 Kharkiv, Ukraine
E-mail: kirichok@bitp.kiev.ua
V M Kuklin V N Karazin Kharkiv National University,
4 Svobody sq., 61022 Kharkiv, Ukraine
E-mail: v.m.kuklin@karazin.ua

Received 7 December 2015
Uspekhi Fizicheskikh Nauk **186** (7) 743 – 762 (2016)
DOI: 10.3367/UFNr.2016.01.037697
Translated by E N Ragozin; edited by A Radzig

Keywords: modulational instability, parametric instability, nonisothermal and cold plasmas, Zakharov's model, Silin's model, hybrid models

1. Introduction

Intense Langmuir waves in plasma, which are easily excited by different sources [1–9], turn out to be parametrically unstable. This instability is responsible for the excitation of a short-wavelength oscillation spectrum synchronized in frequency to the intense Langmuir (pump) wave and for the formation of deep plasma density caverns filled with a high-frequency (HF) field. Interest in these processes was due, in particular, to the opening up of the feasibility of electron and ion heating. The correct tools for describing the parametric instability of long-wavelength Langmuir oscillations were practically developed in the basic work by V P Silin [10] and V E Zakharov [11]. Even the first one-dimensional numerical experiments on the parametric decay of Langmuir oscillations [12] bore out these theoretical predictions [7] (see also Refs [13, 14] and review [15]). The complete theory of parametric plasma oscillation decay was presented in monograph [16] more recently.

However, the pronounced interest of the scientific community was aroused by the effective mechanism of wave energy dissipation discovered and clarified by V E Zakharov — the collapse of Langmuir waves in nonisothermal plasmas [17]. This is the formation of the short-wavelength perturbation spectrum and plasma density caverns, which may be described by Zakharov's equations [17], which were derived with the use of hydrodynamic equations for electron and ion fluids assuming that the energy density of the long-wavelength Langmuir field was lower than the thermal energy density of plasma electrons. In Zakharov's hydrodynamic model, localization domains of short-wavelength Langmuir oscillations emerge. The plasma is forced out of these domains (caverns) under HF radiation pressure, so that the plasma density turns out to be appreciably lower than the volume average density. The subsequent evolution may lead to a so-called collapse — the shrinkage and deepening of the density cavern (the so-called peaking mode). In this case, the cavern shrinkage, as may be seen from more general models describing this phenomenon, should be attended by the electron damping of small-scale HF spectrum modes and the cavern 'collapse' due to HF field burnup (so-called 'physical collapse').

Even early in the study of these processes, analytical investigations as well as hardware and numerical experiments bore out [18–21] the fact that an appreciable energy fraction of intense Langmuir oscillations in a nonisothermal plasma is converted to the energy of the short-wavelength Langmuir spectrum due to modulation instability. A like effect was also discovered in stronger fields in cool plasmas [22, 23], where the field–particle energy transfer mechanism turned out to be similar. This signifies that the nonlinear mechanism of Langmuir oscillation absorption operative when the thermal plasma energy density exceeds the energy density of the HF field, which was discovered by V E Zakharov [17], turned out to be applicable also to fields whose energy density is far greater than the thermal plasma energy. Subsequently, there followed a wealth of papers dedicated to this phenomenon, which is of utmost importance to plasma physics (see, for instance, Refs [24–34]). Special mention should be made of a paper by E A Kuznetsov [35], who most correctly derived Zakharov's model equations describing the modulation instability of Langmuir waves in nonisothermal plasmas. The reader is referred to reviews [36, 37], which give an idea of the scale and efficiency of this research.

The phenomenon of wave energy absorption due to the development of small-scale modulation instability discovered by V E Zakharov has been elaborated in several applications. Many models describing these processes differ from the previous traditional ones, more and more new features are revealed, and new implications of modulation instability development are highlighted.

It is clear that there is no way of including several kinetic effects (for instance, Landau damping) in a hydrodynamic model. That is why use is commonly made of a phenomenological description of this phenomenon by introducing the corresponding terms into the system of hydrodynamic equations. This is admissible to a certain degree, because the nature of Landau damping has been adequately studied. On the other hand, the behavior of particles trapped by a spatially nonuniform field is not quite correctly described by a purely hydrodynamic treatment: their inertia (significant precisely for ions) is in fact ignored. This gives rise not only to deep plasma density caverns of a very small scale, but also to peaking modes, which are not always adequate for the physical reality.

To correctly include Landau damping by electrons, advantage is frequently taken of the kinetic equation for their distribution function. However, it is good to bear in mind that the kinetic damping due to electrons can, under certain conditions, disturb the conditions for modulation instability development by suppressing the field even at the stage of forming caverns which may be distorted in shape in the process. Therefore, there are problems in the interpretation of the process of modulation instability, whose character may markedly change on engaging strong kinetic damping. Furthermore, the kinetic approach, like the hydrodynamic one, describes the motion of a continuous medium and allows the existence of physically unpromising solutions with peakings reaching arbitrarily small scales.

Below, we discuss different models for describing the modulation instability of intense Langmuir oscillations in plasma in a one-dimensional representation. As noted by J M Dawson [38], the choice of one-dimensional models retains the main features of the processes, while significantly simplifying the description and understanding of the physical phenomena. Furthermore, the main difficulty in describing plasma in three-dimensional models is not only the difference in electron and ion masses, but also a very large number of particles (electrons and ions) — on the order of $10^{12}-10^{15}$ or more per unit volume — compeling the construction of rather intricate models, which nevertheless still remain approximate. This hinders the comparison between hydrodynamic, kinetic models and models that use, partly or fully, descriptions with the aid of large particles, particle-in-cell (PIC) method, etc., simulating the behavior of ions and electrons.

In the one-dimensional models corresponding to the three-dimensional case given above, the number of particles corresponding to ions and electrons is on the order of 10^4-10^5 per unit volume, and these particles are therefore close in characteristics to plasma ions and electrons. Therefore, a description involving particles may turn out to be more correct in the framework of a one-dimensional model than a hydrodynamic description or a description based on the kinetic equations for their distribution function. This may permit elucidating the question of the appropriateness of different ways of process description.

1.1 Nonisothermal plasma

The greatest progress was achieved in the study of the modulation instability of an intense Langmuir field in nonisothermal plasmas for a field energy density well below the electron thermal energy density.

In the one-dimensional case, in a nonisothermal plasma a small-scale soliton-like cavern forms, where the HF radiation pressure is balanced by the plasma electron pressure (see, for instance, Ref. [39]). However, it is possible to observe the 'collapse' of plasma density caverns in these low-dimensional cases, too, when the HF pressure lowers due to field burnup caused by Landau damping [40]. Broadly speaking, the cavern collapse maintains the heating of not only electrons but also ions; it increases the entire plasma pressure, which also disturbs the equilibrium state of these structures. In a supersonic mode of cavern wall motion, the probability of a physical collapse may rise even in the one-dimensional case. The modulation instability of an intense Langmuir wave in a nonisothermal plasma has also resulted in collective ion excitations, and in the generation of ion-acoustic waves, in particular [41–44].

A comparison between the one-dimensional Vlasov–Poisson kinetic model, which describes the behavior of electrons and ions with the aid of kinetic equations for the distribution functions, and Zakharov's hydrodynamic model at the same parameter values and the same initial conditions was undertaken, for instance, in Ref. [45], where the amplitude of the long-wavelength field (the pump) did not vary with time. The most adequate was the comparison for the nonisothermal plasma case. In the cavern formation early in the nonlinear process in the constant pump mode, one can see differences in the formation of density caverns whose shape in the kinetic model does not correspond to the perturbation structure typical for the modulation instability. Although in both cases the HF field-induced plasma expulsion gives rise to lower-density domains, the magnitude of density changes in Zakharov's model turned out to be significantly larger than in the Vlasov–Poisson model. Therefore, it was shown that kinetic field damping on plasma particles can distort the modulation instability process and, perhaps, lead to other consequences, in particular, giving rise to groups of fast particles and early disruption of density caverns.

It is highly instructive to compare Zakharov's hydrodynamic model with the model which describes electrons using the kinetic equations for their distribution function and treats ions hydrodynamically [46]. The case of constant pumping was also considered here. This model describes much better the formation of caverns typical for a developed modulation instability, which are hardly different, early in the nonlinear process, from the structures of this kind in Zakharov's hydrodynamic model. A remark is in order regarding the models which apply this kinetic description of the electron plasma component and the hydrodynamic approach to the ion component: not only do they permit describing the formation of plasma density caverns, but they are also able to determine more precisely the characteristics of the electron velocity distribution, in particular, the electron temperature, although they remain unable to provide an answer to questions regarding the ion energy distribution.

In the representation of ions by particles in the framework of the so-called hybrid models[1] (the electrons are described hydrodynamically, and the ions are treated as large particles), ion density fluctuations prove to be quite significant [47–49], at least in the one-dimensional Zakharov's nonisothermal plasma models under discussion. This speeds up the development of modulation instability to the extent that the linear stage of perturbation growth practically escapes observation (although this, as noted below, is due to the fact that the instability increment turns out to be almost the same throughout a wide range of wavenumber values for the supersonic modes of the process under discussion).

A treatment in the framework of such hybrid models would permit taking into account the inertia of ions in the formation and evolution of plasma density caverns, in particular, the mechanism of cavern collapse. It is precisely the direct simulation of the collapse by the particle method that is 'most consistent', in the view of V E Zakharov and his colleagues expressed in Ref. [50]. Indeed, the kinetic and hydrodynamic descriptions operate on objects that are small phase volumes rather than particles, and these phase volumes become arbitrarily small when passing to the classical limit. This leads to a smaller inertia of the substance than in its description by particles.

[1] This name was proposed by Clark et al. [49].

As for the description methods with the aid of large particles in high-dimensional models, this is another extreme. Large particles possess excessive inertia and, therefore, they are quite often replaced with local objects — computation cells — in which the inner contents are averaged. This brings such an approach closer to the hydrodynamic scale description, retaining the features of the large-particle technique and their averaged inertia on a long scale. It is possible to increase the number of model particles in the description, decreasing the fraction (charge and mass) in each of them, although it is hardly possible to approach the real physical parameters in the three-dimensional (3D) space.

In what follows, the emphasis is placed on one-dimensional hybrid models. For one-dimensional simulations, we employ $(2-5)\times 10^4$ model ion-particles (which would correspond to $10^{13}-10^{14}$ such objects in the volume under consideration in the 3D model), with the characteristics of these particles already corresponding to single ions. That is why the dynamics of ion-simulating particles in this case is largely adequate to the dynamics of plasma ions; furthermore, the particle–field energy exchange mechanisms correspond to the real interaction of ions with the low-frequency (LF) oscillation spectrum. This signifies that one-dimensional hybrid models with a large number of particles are able to provide a correct description of the nonlinear Landau damping of slow plasma density perturbations on the ions, leaving beyond the scope of this approach the problems of describing the details of the electron distribution function. The inclusion of the nonresonance interaction of ion-particles with LF spectrum modes and the capture of ions in the potential wells of such oscillations result in an additional instability of density caverns arising due to modulation instability, as well as in the emergence of fast particle groups.

The authors of Ref. [49] undertook a comparison between two models — the hydrodynamic and hybrid Zakharov's — at the same parameter values and the same initial conditions. Because of a higher level of ion density fluctuations, the number of caverns in the hybrid model turned out to be appreciably larger, and they were less deep than in Zakharov's model. The integral characteristics of both models proved to be practically the same. A drawback of the work performed by these authors is a nonself-consistent description, i.e., neglect of the effect of the spectrum under excitation on the pump wave. It should be emphasized that in the cases of description based on the hydrodynamic Zakharov's model [49] and of the description in the framework of kinetic equations for the electron distribution function and hydrodynamic treatment for ions [51], the caverns remained immobile, which was not observed in the hybrid model.

1.2 Cold plasma

With the advent of high-power energy sources, which excited highly intense Langmuir oscillations whose field energy density was far greater than the electron thermal energy density, the model developed by V P Silin [10, 16] and further elaborated by him and his coworkers when describing the parametric instability of an intense field in a cold plasma came into demand. Under these conditions, the dispersion term in the equation for the Langmuir wave field caused by thermal plasma motion is rather small and, assuming the plasma to be cold, may be ignored in many cases.

Indeed, when the field energy density is appreciably higher than the plasma thermal energy density, modulation instability develops, at least early in the process, according to the scenario proposed by Silin et al. [10, 22], in whose models a powerful Langmuir wave in a cold plasma induces intense electron velocity oscillations whose amplitude is comparable to the wavelength of the modes of the spectrum under excitation. In this case, generally speaking, the instability should be termed parametric [16]. Both Zakharov's and Silin's models nevertheless turn out to be physically similar [52]. This is precisely why the term 'modulation instability' applies to the description of the instability of the powerful Langmuir field in Silin's model as well.

Notably, even in one-dimensional numerical simulations of the process, proceeding from the hydrodynamic Silin equations generalized in Refs [53, 54], the modulation instability developed and a partial energy exchange occurred between its short-wavelength spectrum and an intense pump wave. The results of such simulations are in qualitative and quantitative agreement with the results of numerical experiments performed earlier at the P N Lebedev Physical Institute [22]. A peaking mode, which was characterized by a shortening of the cavern scale length and simulation breakdown, could be observed. It is the latter circumstance that compelled us to move to a description of ions as particles.

In the hybrid Silin model (electrons are hydrodynamically described, and ions are treated as large particles), in precisely the same way density caverns formed, which then collapsed [48]. This was caused not only by the nonequilibrium initial state of the caverns (due to violation of the balance between the HF pressure and the plasma pressure) and the field burnup effect, but also by the inclusion of inertia of ion-simulating particles whose number was not large enough in the numerical experiments. In this case, the ion cavern 'collapsed' and the ion component passed into the particle trajectory crossing mode [47, 48]. The energy extracted by the ions was on the order of $(m_e/M)^{1/3}$ fraction of the initial energy of the pump wave [48] (here, m_e and M are the electron and ion masses, respectively). For electrons, the passage to the trajectory crossing mode could be restrained by the existence of the ion cavern, which was capable of synchronizing the ejection of fast electrons and ions at the instant of its collapse. Experiments were made to produce — in the vicinity of the plasma resonance in a nonuniform plasma — a close-to-Langmuir-frequency field with a high energy density W exceeding the plasma thermal energy density $n_{e0}T_{e0}$. These experiments demonstrated the generation of short fast-particle pulses against the background of electron heating in the vicinity of the plasma resonance. In this case, the energy was removed from the domain of plasma resonance not only by electrons, but also by ions [55–57] of rather high energy (see, for instance, review [57]). The domains of electron pulse sources corresponded to the small dimensions of the plasma density caverns. The energy fraction stored in the fast ions after the cavern collapse was roughly consistent with the theoretical values given in Refs [48, 58–60].

In the literature, the instability of oscillatory electron motion at the Langmuir frequency relative to immobile ions was quite often referred to as the oscillatory Buneman instability. The similarity between the Buneman instability and the Langmuir wave instability in a cold plasma is attested to by the fact that the increments and the initial velocities of the relative motion of electrons and ions are approximately equal. An analysis of Buneman instability development was outlined in monograph [6], where a lowering of the velocity (current disruption) of the relative motion and a growth of perturbations of the electron and ion components were observed at the nonlinear stage of the process. This is in qualitative correspondence with the processes occurring in the development of the parametric instability of an intense Langmuir wave in a cold plasma.

The parametric instability of Langmuir waves under the applicability conditions of Zakharov's equations and Silin's equations was usually discussed by theorists separately, although quite often these processes were not distinguished in experiments. It would therefore be instructive to compare the behavior of the parametric instability of intense Langmuir oscillations in hot and cold plasmas in the framework of hybrid self-consistent models. The bulk of attention was directed towards the behavior of the ion plasma component. It turned out that the HF field energy fraction transferred to ions in the nonisothermal plasma was on the order of W/n_0T_{e0}, while in the cold plasma case an estimate [48] on the order of $(m_e/M)^{1/3}$ was confirmed. In the latter case, the fraction of fast particles in their energy distribution turned out to be larger [58–60].

In our paper, special emphasis is also placed on a comparison of the character of exciting the collective degrees of freedom in low-frequency motions, particularly, of the generation of ion waves in the hybrid Zakharov and Silin models. It is also important to elucidate how the rate of HF field burnup in plasma caverns affects the character of ion dynamics. These and other questions are discussed below.

1.3 Comparison between Zakharov's and Silin's models

The main objective of this paper is to discuss different one-dimensional models in order to describe the modulation instability of intense long-wavelength Langmuir oscillations and to elucidate the features of energy transfer to ions and collective ion perturbations in nonisothermal and cold plasmas [59–61].

As shown below, the description of the parametric instability of the intense long-wavelength Langmuir field in plasmas with the excitation of a short-wavelength Langmuir oscillation spectrum is universal both for a cold plasma (i.e., when the field energy density exceeds the thermal energy density of the medium, $W = |E_0|^2/4\pi \gg n_0T_e$) and for a nonisothermal plasma (when the plasma thermal energy density exceeds the field energy density, $W = |E_0|^2/4\pi \ll n_0T_e$, where E_0 is the initial strength of the long-wavelength Langmuir wave field, n_0 is the unperturbed plasma density, T_e is the electron temperature, and the ions are assumed to be cold). To obtain the systems of equations for each of Silin's and Zakharov's models, we therefore take advantage of the approach outlined in V P Silin's book [16].

Although the Silin and Zakharov models under discussion were intended for different physical conditions, constructed relatively long ago, and developed independently for a long time, there has so far been no clear understanding of the close relationship between them. In this study, we endeavored to demonstrate this relationship and highlight the similarity of the physical mechanisms underlying the phenomena described by these models, which is important, in particular, from the methodological standpoint.

2. Cold plasma: one-dimensional Silin equations

First, let us consider the development of parametric instability of an external high-intensity long-wavelength Langmuir field for a cold plasma, i.e., when the field energy density exceeds the thermal energy density of the medium: $W = |E_0|^2/4\pi \gg n_0 T_e$. The quasihydrodynamic equations for particles of sort α are given in the form [16]

$$\frac{\partial v_\alpha}{\partial t} + u_{0\alpha}\frac{\partial}{\partial x} v_\alpha - \frac{e_\alpha}{m_\alpha} E = -v_\alpha \frac{\partial}{\partial x} v_\alpha\,, \tag{2.1}$$

$$\frac{\partial n_\alpha}{\partial t} + u_{0\alpha}\frac{\partial}{\partial x} n_\alpha + n_{0\alpha}\frac{\partial}{\partial x} v_\alpha = -\frac{\partial}{\partial x}(n_\alpha v_\alpha)\,, \tag{2.2}$$

$$\frac{\partial}{\partial x} E = 4\pi \sum_\beta e_\beta n_\beta\,, \tag{2.3}$$

where $\alpha = \mathrm{e}$ and $\alpha = \mathrm{i}$ stand for electrons and ions, respectively.

The particles are in the field of an external wave (its wavelength is assumed to be infinite for simplicity of calculations) and oscillate with a velocity $u_{0\alpha} = -(e_\alpha|E_0|/m_\alpha\omega_0)\cos\Phi$.

The components of the external wave field strength are defined as follows:

$$E_0 = -\frac{\mathrm{i}}{2}\left[|E_0|\exp(\mathrm{i}\omega_0 t + \mathrm{i}\phi) - |E_0|\exp(-\mathrm{i}\omega_0 t - \mathrm{i}\phi)\right]. \tag{2.4}$$

Eliminating

$$E_n = -\frac{4\pi\mathrm{i}e(n_{\mathrm{i},n} - n_{\mathrm{e},n})}{k_0 n}\,,$$

in the Fourier representation we rewrite the first equation of system (2.1)–(2.3) in the following form

$$\frac{\partial v_{\alpha,n}}{\partial t} + u_{0\alpha}\mathrm{i}k_0 n v_{\alpha,n} + \frac{4\pi e_\alpha \mathrm{i}}{k_0 n m_\alpha}\sum_\beta e_\beta n_{\beta,n} = -\mathrm{i}k_0 \sum_m m v_{\alpha,n-m} v_{\alpha,m}\,. \tag{2.5}$$

Below, we take advantage of the following variables

$$\nu_{\alpha,n} = e_\alpha n_{\alpha,n}\exp(-\mathrm{i}a_{\alpha,n}\sin\Phi)\,, \tag{2.6}$$

$$\theta_{\alpha,n} = v_{\alpha,n}\exp(-\mathrm{i}a_{\alpha,n}\sin\Phi)\,, \tag{2.7}$$

where

$$a_{\alpha,n} = \frac{n e_\alpha k_0 E_0}{m_\alpha \omega_0^2}\,, \qquad \Phi = \omega_0 t + \phi\,. \tag{2.8}$$

In this case, Eqns (2.1) and (2.2) may be written out as

$$\frac{\partial \nu_{\alpha,n}}{\partial t} + \theta_{\alpha,n}\mathrm{i}k_0 n e_\alpha n_{\alpha,0} = -\mathrm{i}k_0 n \sum_m \nu_{\alpha,n-m}\theta_{\alpha,m}\,, \tag{2.9}$$

$$\frac{\partial \theta_{\alpha,n}}{\partial t} + \frac{4\pi e_\alpha \mathrm{i}}{k_0 n m_\alpha}\sum_\beta \nu_{\beta,n}\exp\left[\mathrm{i}(a_{\beta,n} - a_{\alpha,n})\sin\Phi\right] = -\mathrm{i}k_0 \sum_m m\theta_{\alpha,n-m}\theta_{\alpha,m}\,. \tag{2.10}$$

It is evident that $a_{\mathrm{i},n} - a_{\mathrm{e},n} = n(ek_0E_0/M\omega_0^2) + n(ek_0E_0/m_\mathrm{e}\omega_0^2) \approx n(ek_0E_0/m_\mathrm{e}\omega_0^2) = a_n$, where the quantity $k_n = nk_0$ defines the discrete set of the wavenumbers of the short-wavelength spectrum modes. For electrons, Eqns (2.9) and (2.10) may be written out in the form

$$\frac{\partial \nu_{\mathrm{e},n}}{\partial t} - \theta_{\mathrm{e},n}\mathrm{i}k_0 n e n_0 = -\mathrm{i}k_0 n \sum_m \nu_{\mathrm{e},n-m}\theta_{\mathrm{e},m}\,, \tag{2.11}$$

$$\frac{\partial \theta_{\mathrm{e},n}}{\partial t} - \frac{4\pi e\mathrm{i}}{k_0 n m_\mathrm{e}}\left(\nu_{\mathrm{e},n} + \nu_{\mathrm{i},n}\exp(\mathrm{i}a_n\sin\Phi)\right) = -\mathrm{i}k_0 \sum_m m\theta_{\mathrm{e},n-m}\theta_{\mathrm{e},m}\,. \tag{2.12}$$

We resort to the representation

$$\nu_{\mathrm{e},n} = \sum_s u_n^{(s)}\exp(\mathrm{i}s\omega_0 t) = u_n^{(0)} + u_n^{(1)}\exp(\mathrm{i}\omega_0 t) + u_n^{(-1)}\exp(-\mathrm{i}\omega_0 t) + u_n^{(2)}\exp(\mathrm{i}2\omega_0 t) + u_n^{(-2)}\exp(-\mathrm{i}2\omega_0 t)\,, \tag{2.13}$$

$$\theta_{\mathrm{e},n} = \sum_s \upsilon_n^{(s)}\exp(\mathrm{i}s\omega_0 t) = \upsilon_n^{(0)} + \upsilon_n^{(1)}\exp(\mathrm{i}\omega_0 t) + \upsilon_n^{(-1)}\exp(-\mathrm{i}\omega_0 t) + \upsilon_n^{(2)}\exp(\mathrm{i}2\omega_0 t) + \upsilon_n^{(-2)}\exp(-\mathrm{i}2\omega_0 t)\,, \tag{2.14}$$

and to the well-known expansion

$$\exp(\mathrm{i}a\sin\Phi) = \sum_{m=-\infty}^{\infty} J_m(a)\exp(\mathrm{i}m\Phi)\,, \tag{2.15}$$

where $J_m(x)$ is the Bessel function with $J_0(x) = J_0(-x)$, $J_1(x) = -J_1(-x) = J_{-1}(-x)$, and $J_2(x) = J_{-2}(x) = J_2(-x)$ [39]. After that, we find the nonresonant density perturbations $u_n^{(0)}$, $u_n^{(2)}$, and $u_n^{(-2)}$ and velocity perturbations $\upsilon_n^{(0)}$, $\upsilon_n^{(2)}$, and $\upsilon_n^{(-2)}$ in the oscillating frame of reference:

$$\upsilon_n^{(0)} = \frac{k_0}{\omega_0}\sum_m (n-m)\left[\upsilon_{n-m}^{(1)}\upsilon_m^{(-1)} - \upsilon_{n-m}^{(-1)}\upsilon_m^{(1)}\right] = \frac{1}{\mathrm{i}\omega_0}\left[\frac{\partial \upsilon^{(1)}}{\partial x}\upsilon^{(-1)} - \frac{\partial \upsilon^{(-1)}}{\partial x}\upsilon^{(1)}\right]_n\,, \tag{2.16}$$

$$u_n^{(0)} = -\nu_{\mathrm{i},n}J_0(a_n) + \frac{k_0^2 n^2 m_\mathrm{e}}{4\pi e}\sum_m \upsilon_{n-m}^{(1)}\upsilon_m^{(-1)} = -\nu_{\mathrm{i},n}J_0(a_n) - \frac{m_\mathrm{e}}{4\pi e}\left[\frac{\partial^2}{\partial x^2}\left(\upsilon^{(1)}\upsilon^{(-1)}\right)\right]_n\,, \tag{2.17}$$

$$\upsilon_n^{(\pm 2)} = \pm\frac{2\omega_0}{3k_0 n e n_0}\,\nu_{\mathrm{i},n}J_{\pm 2}(a_n)\exp(\pm 2\mathrm{i}\phi) \mp \frac{k_0}{\omega_0}\sum_m m\upsilon_{n-m}^{(\pm 1)}\upsilon_m^{(\pm 1)} = \pm\frac{2\omega_0}{3k_0 n e n_0}\,\nu_{\mathrm{i},n}J_{\pm 2}(a_n)\exp(\pm 2\mathrm{i}\phi) \mp \frac{1}{\mathrm{i}\omega_0}\left[\frac{\partial \upsilon^{(\pm 1)}}{\partial x}\upsilon^{(\pm 1)}\right]_n\,, \tag{2.18}$$

$$u_n^{(\pm 2)} = \frac{1}{3}\,\nu_{\mathrm{i},n}J_{\pm 2}(a_n)\exp(\pm 2\mathrm{i}\phi) - \frac{k_0^2 n e n_0}{\omega_{pe}^2}\sum_s s\upsilon_s^{(\pm 1)}\upsilon_{n-s}^{(\pm 1)} = \frac{1}{3}\,\nu_{\mathrm{i},n}J_{\pm 2}(a_n)\exp(\pm 2\mathrm{i}\phi) + \frac{e n_0}{\omega_{\mathrm{pe}}^2}\left[\frac{\partial}{\partial x}\left(\frac{\partial \upsilon^{(\pm 1)}}{\partial x}\upsilon^{(\pm 1)}\right)\right]_n. \tag{2.19}$$

Expressions (2.16) and (2.17), which are proportional to $J_0(a_n)$, correspond to slow motions, while expressions (2.18) and (2.19), which are proportional to $J_{\pm 2}(a_n)$, are determined by the contribution from the second harmonic to the nonlinearity.

In Refs [52, 53], use was made of the representation $u_n^{(\pm 1)} = \pm k_0 n e n_0 \upsilon_n^{(\pm 1)}/\omega_0 = \mathrm{i}k_0 n E_n^{(\pm 1)}/4\pi$, where $\upsilon_n^{(\pm 1)} = \pm\mathrm{i}eE_n^{(\pm 1)}/m\omega_0$. In this case, we collect on the right-hand side the terms responsible only for electron nonlinearity to obtain the equation for short-wavelength perturbations in the following form

$$\pm 2\mathrm{i}\omega_0\left[\frac{\partial u_n^{(\pm1)}}{\partial t} \mp \mathrm{i}\,\frac{\omega_{pe}^2-\omega_0^2}{2\omega_0}\,u_n^{(\pm1)} \mp \mathrm{i}\nu_{\mathrm{i},n}\,\frac{\omega_{pe}^2 J_{\pm1}(a_n)\exp(\pm\mathrm{i}\phi)}{2\omega_0}\right]\exp(\pm\mathrm{i}\omega_0 t)$$
$$+\frac{\omega_0^2}{en_0}\,n\exp(\pm\mathrm{i}\omega_0 t)\sum_m \frac{\nu_{\mathrm{i},n-m}}{m}\left[u_m^{(\mp1)}J_{\pm2}(a_{n-m})\exp(\pm2\mathrm{i}\phi) + u_m^{(\pm1)}J_0(a_{n-m})\right] = \frac{k_0 n e n_0}{\omega_0}\,I\,, \qquad (2.20)$$

where the electron nonlinearity contribution I may be written out as

$$I = -\frac{\partial}{\partial x}\left(v^{(\pm1)}\left[\frac{\partial v^{(1)}}{\partial x}\,v^{(-1)} - \frac{\partial v^{(-1)}}{\partial x}\,v^{(1)}\right]\right) \mp v^{(\pm1)}\,\frac{\partial^2}{\partial x^2}\left[v^{(1)}v^{(-1)}\right] - \frac{\partial v^{(\pm1)}}{\partial x}\left[\frac{\partial v^{(1)}}{\partial x}\,v^{(-1)} - \frac{\partial v^{(-1)}}{\partial x}\,v^{(1)}\right]$$
$$\pm v^{(\mp1)}\,\frac{\partial}{\partial x}\left[\frac{\partial v^{(\pm1)}}{\partial x}\,v^{(\pm1)}\right] \pm v^{(\mp1)}\,\frac{\partial}{\partial x}\left[\frac{\partial v^{(\pm1)}}{\partial x}\,v^{(\pm1)}\right].$$

It is evident that the right-hand side of Eqn (2.20), which corresponds to the contribution of electron nonlinearity in the one-dimensional case under consideration, is equal to zero, which was independently noted in V P Silin's [10, 15] and V E Zakharov's [11] work earlier.

If the resonant field is represented in the form $(E_n^{(1)}\exp(\mathrm{i}\omega_0 t) + E_n^{(-1)}\exp(-\mathrm{i}\omega_0 t))/2$, as was done in E A Kuznetsov's work [35] [see Eqn (3.10) below], then $E_n^{(\pm1)} \to E_n^{(\pm1)}/2 = -4\pi\mathrm{i}u_n^{(\pm1)}/k_0 n$ and Eqn (2.20) may be written out differently:

$$\frac{\partial E_n^{(\pm1)}}{\partial t} \mp \mathrm{i}\,\frac{\omega_{pe}^2-\omega_0^2}{2\omega_0}\,E_n^{(\pm1)} \mp \frac{8\pi\omega_{pe}\nu_{\mathrm{i},n}}{2k_0 n}\,J_{\pm1}(a_n)\exp(\pm\mathrm{i}\phi) \mp \mathrm{i}\,\frac{\omega_0}{2en_0}\sum_m \nu_{\mathrm{i},n-m}\left[E_m^{(\mp1)}J_{\pm2}(a_{n-m})\exp(\pm2\mathrm{i}\phi) + E_m^{(\pm1)}J_0(a_{n-m})\right] = 0\,. \qquad (2.21)$$

The equation for the pump wave is also given by:

$$\frac{\partial E_0^{(\pm1)}}{\partial t} \mp \mathrm{i}\,\frac{\omega_{pe}^2-\omega_0^2}{2\omega_0}\,E_0^{(\pm1)} \mp \frac{8\pi\omega_0}{2en_0k_0}\sum_m \frac{\nu_{\mathrm{i},-m}}{m}\left[u_m^{(\mp1)}J_{\pm2}(a_{-m})\exp(\pm2\mathrm{i}\phi) + u_m^{(\pm1)}J_0(a_{-m})\right] = 0\,. \qquad (2.22)$$

From the pump wave representation corresponding to the selected oscillation velocity $u_{0\alpha} = -(e_\alpha E_0/m_\alpha\omega_0)\cos\Phi$, we obtain[2] $E_0 \to -\mathrm{i}E_0$ and $E_0^* \to \mathrm{i}E_0^*$, and Eqn (2.22) for E_0 may be rewritten [52] by expressing the density perturbations in terms of the electric field strengths of the modes:

$$\frac{\partial E_0}{\partial t} - \mathrm{i}\Delta E_0 = -\frac{\omega_0}{2en_0}\sum_m \nu_{\mathrm{i},-m}\left[E_m^{(-1)}J_2(a_m)\exp(2\mathrm{i}\phi) + E_m^{(+1)}J_0(a_m)\right], \qquad (2.23)$$

where $\Delta = (\omega_{pe}^2 - \omega_0^2)/2\omega_0$. Here, again, the terms proportional to $J_0(a_n)$ on the right-hand side of Eqn (2.23) correspond to slow motions, while the terms proportional to $J_{\pm2}(a_n)$ are determined by the contribution of the second harmonic to the nonlinearity.

The slowly time-varying electric field strength may be represented as

$$\bar{E}_n = -\frac{4\pi\mathrm{i}}{k_0 n}\,\nu_{\mathrm{i},n}\left[1 - J_0^2(a_n) + \frac{2}{3}\,J_2^2(a_n)\right] + \frac{1}{2}\left[E_n^{(1)}J_1(a_n)\exp(-\mathrm{i}\phi) + E_n^{(-1)}J_{-1}(a_n)\exp(\mathrm{i}\phi)\right] - \frac{\mathrm{i}nk_0}{16\pi en_0}\,J_0(a_n)\sum_m E_{n-m}^{(1)}E_m^{(-1)}$$
$$- \frac{\mathrm{i}k_0}{16\pi en_0}\,J_2(a_n)\sum_m (n-m)\left[E_{n-m}^{(1)}E_m^{(1)}\exp(-2\mathrm{i}\phi) + E_{n-m}^{(-1)}E_m^{(-1)}\exp(2\mathrm{i}\phi)\right]. \qquad (2.24)$$

This permits describing ions by large particles, whose equations of motion are of the form

$$\frac{\mathrm{d}^2x_s}{\mathrm{d}t^2} = \frac{e}{M}\sum_n \bar{E}_n\exp(\mathrm{i}k_0 n x_s)\,, \qquad (2.25)$$

and the ion density is defined by the relationships

$$\nu_{\mathrm{i},n} = en_{\mathrm{i},n} = en_0\,\frac{k_0}{2\pi}\int_{-\pi/k_0}^{\pi/k_0}\exp\left(-\mathrm{i}nk_0 x_s(x_{s0},t)\right)\mathrm{d}x_{s0}\,. \qquad (2.26)$$

It should be noted that the description of ions as large particles, as shown in Ref. [48], permits, among other things, improving the stability of the numerical computation scheme. Using Eqns (2.9) and (2.10), in which the right-hand sides may be ignored due to their smallness, it is possible to move to a hydrodynamic ion description. In this case, the equation for the ion density assumes the form [52]

$$\frac{\partial^2\nu_{\mathrm{i},n}}{\partial t^2} = -\Omega_{\mathrm{i}}^2\left\{\nu_{\mathrm{i},n}\left[1 - J_0^2(a_n) + \frac{2}{3}\,J_2^2(a_n)\right] + \frac{\mathrm{i}k_0 n}{8\pi}\left[E_n^{(1)}J_1(a_n)\exp(-\mathrm{i}\phi) + E_n^{(-1)}J_{-1}(a_n)\exp(\mathrm{i}\phi)\right] + \frac{n^2k_0^2}{64\pi^2 en_0}\sum_m J_0(a_n)E_{n-m}^{(1)}E_m^{(-1)}\right.$$
$$\left. + \frac{nk_0^2}{64\pi^2 en_0}\,J_2(a_n)\sum_m (n-m)\left[E_{n-m}^{(1)}E_m^{(1)}\exp(-2\mathrm{i}\phi) + E_{n-m}^{(-1)}E_m^{(-1)}\exp(2\mathrm{i}\phi)\right]\right\}. \qquad (2.27)$$

As is easily verified, for the lower sign the complex-conjugate Eqn (2.22) takes on the form (in the summation,

[2] This practically implies that $|E_0|\exp(\mathrm{i}\phi) \to |E_0|\exp(\mathrm{i}\phi - \mathrm{i}\pi/2)$, since the phase $\phi_0 = \mathrm{i}\pi/2$ is related to the choice of the form of the oscillation velocity.

the umbral index may be replaced, $m \to -m$)

$$\frac{\partial (E_{-n}^{(-1)})^*}{\partial t} - \mathrm{i}\,\frac{\omega_{pe}^2 - \omega_0^2}{2\omega_0}(E_{-n}^{(-1)})^* - \frac{4\pi\omega_{pe} v_{\mathrm{i},-n}^*}{k_0 n} J_1(a_n)\exp(\mathrm{i}\phi)$$
$$- \mathrm{i}\,\frac{\omega_0}{2en_0}\sum_m v_{\mathrm{i},-n+m}^*\big[(E_{-m}^{(1)})^* J_{-2}(a_{-n+m})\exp(2\mathrm{i}\phi)$$
$$+ (E_{-m}^{(-1)})^* J_0(a_{-n+m})\big] = 0\,. \tag{2.28}$$

At the same time, for positive indices this equation may be written out as

$$\frac{\partial E_n^{(1)}}{\partial t} - \mathrm{i}\,\frac{\omega_{pe}^2 - \omega_0^2}{2\omega_0} E_n^{(1)} - \frac{4\pi\omega_{pe} v_{\mathrm{i},n}}{k_0 n} J_{\pm 1}(a_n)\exp(\mathrm{i}\phi)$$
$$- \mathrm{i}\,\frac{\omega_0}{2en_0}\sum_m v_{\mathrm{i},n-m}\big[E_m^{(-1)} J_2(a_{n-m})\exp(2\mathrm{i}\phi)$$
$$+ E_m^{(1)} J_0(a_{n-m})\big] = 0\,. \tag{2.29}$$

It is easy to see that Eqns (2.28) and (2.29) are identical at $E_{-n}^{(-1)} = (E_n^{(1)})^*$ and $v_{\mathrm{i},-n} = v_{\mathrm{i},n}^*$. In precisely the same way, it may be verified that similar transformations yield $E_n^{(-1)} = (E_{-n}^{(1)})^*$ and $v_{\mathrm{i},n} = v_{\mathrm{i},-n}^*$. The ion charge perturbations possess symmetry: $n_{\mathrm{i},-n} = n_{\mathrm{i},n}^*$. In this case, to correctly describe the instability process, it would suffice to use the HF field components $E_n^{(1)}$, $E_{-n}^{(1)}$, and $E_0^{(1)}$, as well as the ion charge perturbations $v_{\mathrm{i},n}$ for positively defined values of index n. This can be done, since the remaining quantities are expressed in terms of them, i.e., it is possible to abandon the use of the upper index. Under these conditions, the systems of equations of the hydrodynamic (2.21), (2.23), (2.27) and hybrid (2.21), (2.23), (2.26) models can be written out in the form as follows.

2.1 Equations of Silin's hydrodynamic model under the conditions $W = |E_0|^2/4\pi \gg n_0 T_e$

In this case, the equations have the form

$$\frac{\partial E_n}{\partial t} - \mathrm{i}\left(\frac{\omega_{pe}^2 - \omega_0^2}{2\omega_0} + \beta n^2\right)E_n + \theta\,\frac{n^6}{n_M^6}\,E_n$$
$$- \frac{4\pi\omega_{pe} v_{\mathrm{i},n}}{k_0 n} J_1(a_n)\exp(\mathrm{i}\phi)$$
$$- \mathrm{i}\,\frac{\omega_0}{2en_0}\sum_m v_{\mathrm{i},n-m}\big[E_{-m}^* J_2(a_{n-m})\exp(2\mathrm{i}\phi) + E_m J_0(a_{n-m})\big] = 0\,,$$

$$\frac{\partial^2 v_{\mathrm{i},n}}{\partial t^2} = -\Omega_{\mathrm{i}}^2\left\{v_{\mathrm{i},n}\left[1 - J_0^2(a_n) + \frac{2}{3}\,J_2^2(a_n)\right]\right.$$
$$+ \frac{\mathrm{i}k_0 n}{8\pi} J_1(a_n)\big[E_n\exp(-\mathrm{i}\phi) - E_{-n}^*\exp(\mathrm{i}\phi)\big]$$
$$+ \frac{n^2 k_0^2}{64\pi^2 e n_0} J_0(a_n)\sum_m E_{n-m}E_{-m}^*$$
$$+ \frac{n k_0^2}{64\pi^2 e n_0} J_2(a_n)\sum_m (n-m)\big[E_{n-m}E_m\exp(-2\mathrm{i}\phi)$$
$$\left. + E_{m-n}^* E_{-m}^*\exp(2\mathrm{i}\phi)\big]\right\}, \tag{2.30}$$

$$\frac{\partial E_0}{\partial t} - \mathrm{i}\Delta E_0$$
$$= -\frac{\omega_0}{2en_0}\sum_m v_{\mathrm{i},-m}\big[E_{-m}^* J_2(a_m)\exp(2\mathrm{i}\phi) + E_m J_0(a_m)\big]\,.$$

2.2 Equations of Silin's hybrid model under the conditions $W = |E_0|^2/4\pi \gg n_0 T_e$

In this case, the equations take on the form

$$\frac{\partial E_n}{\partial t} - \mathrm{i}\left(\frac{\omega_{pe}^2 - \omega_0^2}{2\omega_0} + \beta n^2\right)E_n$$
$$+ \theta\,\frac{n^6}{n_M^6}\,E_n - \frac{4\pi\omega_{pe} v_{\mathrm{i},n}}{k_0 n} J_1(a_n)\exp(\mathrm{i}\phi)$$
$$- \mathrm{i}\,\frac{\omega_0}{2en_0}\sum_m v_{\mathrm{i},n-m}\big[E_{-m}^* J_2(a_{n-m})\exp(2\mathrm{i}\phi) + E_m J_0(a_{n-m})\big] = 0\,,$$

$$\bar{E}_n = -\frac{4\pi\mathrm{i}}{k_0 n}\,v_{\mathrm{i},n}\left[1 - J_0^2(a_n) + \frac{2}{3}\,J_2^2(a_n)\right]$$
$$+ \frac{1}{2}\,J_1(a_n)\big[E_n\exp(-\mathrm{i}\phi) - E_{-n}^*\exp(\mathrm{i}\phi)\big]$$
$$- \frac{\mathrm{i}nk_0}{16\pi e n_0} J_0(a_n)\sum_m E_{n-m}E_{-m}^*$$
$$- \frac{\mathrm{i}k_0}{16\pi e n_0} J_2(a_n)\sum_m (n-m)\big[E_{n-m}E_m\exp(-2\mathrm{i}\phi)$$
$$+ E_{m-n}^* E_{-m}^*\exp(2\mathrm{i}\phi)\big]\,,$$

$$\frac{\mathrm{d}^2 x_s}{\mathrm{d}t^2} = \frac{e}{M}\sum_n \bar{E}_n\exp(\mathrm{i}k_0 n x_s)\,, \tag{2.31}$$

$$v_{\mathrm{i},n} = en_0\,\frac{k_0}{2\pi}\int_{-\pi/k_0}^{\pi/k_0}\exp\big(-\mathrm{i}nk_0 x_s(x_{s0},t)\big)\,\mathrm{d}x_{s0}\,,$$

$$\frac{\partial E_0}{\partial t} - \mathrm{i}\Delta E_0$$
$$= -\frac{\omega_0}{2en_0}\sum_m v_{\mathrm{i},-m}\big[E_{-m}^* J_2(a_m)\exp(2\mathrm{i}\phi) + E_m J_0(a_m)\big]\,.$$

The term $\theta(n/n_M)^6 E_n$ in the first equations of systems (2.30) and (2.31) models the damping of HF spectrum modes on electrons, with $n_M = 20$ and $\Delta = (\omega_{pe}^2 - \omega_0^2)/2\omega_0$. Furthermore, a dispersion term proportional to $\beta = k_0^2 v_{Te}^2/2\omega_0$ was added to the first equations of systems (2.30) and (2.31).

3. Nonisothermal plasma: one-dimensional Zakharov equations

Let us derive the equations describing the instability of intense long-wavelength Langmuir field in a nonisothermal plasma with the excitation of a short-wavelength Langmuir oscillation spectrum, when the thermal energy density of the plasma exceeds the field energy density: $W = |E_0|^2/4\pi \ll n_0 T_e$ (the so-called Zakharov model). The plasma electron behavior may be described hydrodynamically, when the phase velocities of the Langmuir waves exceed the electron thermal velocity. The ions may also be described both hydrodynamically and as large particles. As noted above, these equations were set up most correctly in Ref. [35]. Below, however, for generality of treatment we take advantage of V P Silin's approach outlined in monograph [16], which was employed in Refs [52, 53] to describe the parametric instability of intense long-wavelength Langmuir field in plasmas.

We restrict ourselves to a one-dimensional treatment. In this case, the electron velocity v_e and density n_e obey the following equations:

$$\frac{\partial v_e}{\partial t} + \frac{e}{m_e}\,E + \frac{1}{m_e n_e}\frac{\partial P_e}{\partial x} = -v_e\,\frac{\partial}{\partial x}\,v_e\,, \tag{3.1}$$

$$\frac{\partial n_{\rm e}}{\partial t}+n_0\,\frac{\partial}{\partial x}\,v_{\rm e}=-\frac{\partial}{\partial x}\,(n_{\rm e}v_{\rm e})\,,\qquad(3.2)$$

$$\frac{\partial}{\partial x}\,E=4\pi e(n_{\rm i}-n_{\rm e})\,,\qquad(3.3)$$

where $E=-\,\partial\phi/\partial x$, E and ϕ are the oscillation electric field strength and potential, $P_{\rm e}=n_{\rm e}T_{\rm e}$ is the pressure, $T_{\rm e}$ is the electron temperature in energy units, $v_{T{\rm e}}=\sqrt{T_{\rm e}/m_{\rm e}}$ is the electron thermal velocity, $n_{\rm i}$ is the density of plasma ions, and n_0 is the unperturbed density of both the electrons and the ions.

We express the electric field as a series expansion

$$E=\sum_n E_n\exp\,({\rm i}k_nx)=\sum_n E_n\exp\,({\rm i}nk_0x)\,,$$

where the quantity $k_n=nk_0$ defines the discrete set of spectrum mode wavenumbers.

Rewriting Eqns (3.1) and (3.2) gives

$$\frac{\partial v_{{\rm e},\,n}}{\partial t}-\frac{e}{m_{\rm e}}\,E_n+\frac{v_{T{\rm e}}^2}{n_0}\,{\rm i}k_0nn_{\rm e}=-{\rm i}k_0\sum_m mv_{{\rm e},\,n-m}v_{{\rm e},\,m}\,,\qquad(3.4)$$

$$\frac{\partial n_{{\rm e},\,n}}{\partial t}+n_0{\rm i}k_0nv_{{\rm e},\,n}=-{\rm i}k_0n\sum_m n_{{\rm e},\,n-m}v_{{\rm e},\,m}\,,\qquad(3.5)$$

$${\rm i}k_0nE_n=4\pi e(n_{{\rm i},\,n}-n_{{\rm e},\,n})\,.\qquad(3.6)$$

Eliminating $E_n=-4\pi{\rm i}e(n_{{\rm i},\,n}-n_{{\rm e},\,n})/k_0n$ brings Eqn (3.4) in the form

$$\frac{\partial v_{{\rm e},\,n}}{\partial t}=\frac{4\pi e^2{\rm i}}{k_0nm_{\rm e}}\,(n_{{\rm i},\,n}-n_{{\rm e},\,n})-\frac{v_{T{\rm e}}^2}{n_0}\,{\rm i}k_0nn_{\rm e}-{\rm i}k_0\sum_m mv_{{\rm e},\,n-m}v_{{\rm e},\,m}\,.\qquad(3.7)$$

Following Ref. [14], we represent the electron density and velocity, as was done in Ref. [35], in the form

$$-\,en_{{\rm e},\,n}=\sum_s u_n^{(s)}\exp\,({\rm i}s\omega_0t)=u_n^{(0)}+u_n^{(1)}\exp\,({\rm i}\omega_0t)$$
$$+\,u_n^{(-1)}\exp\,(-{\rm i}\omega_0t)+u_n^{(2)}\exp\,({\rm i}2\omega_0t)+u_n^{(-2)}\exp\,(-{\rm i}2\omega_0t)\,,\qquad(3.8)$$

$$v_{{\rm e},\,n}=\sum_s v_n^{(s)}\exp\,({\rm i}s\omega_0t)=v_n^{(0)}+v_n^{(1)}\exp\,({\rm i}\omega_0t)$$
$$+\,v_n^{(-1)}\exp\,(-{\rm i}\omega_0t)+v_n^{(2)}\exp\,({\rm i}2\omega_0t)+v_n^{(-2)}\exp\,(-{\rm i}2\omega_0t)\,,\qquad(3.9)$$

$$E_n=\sum_s E_n^{(s)}\exp\,({\rm i}s\omega_0t)=\bar{E}_n+E_n^{(1)}\exp\,({\rm i}\omega_0t)$$
$$+\,E_n^{(-1)}\exp\,(-{\rm i}\omega_0t)+E_n^{(2)}\exp\,({\rm i}2\omega_0t)+E_n^{(-2)}\exp\,(-{\rm i}2\omega_0t)\,.\qquad(3.10)$$

We take advantage of the linear relationships $u_{n-m}^{(\pm1)}=\pm k_0(n-m)en_0\omega_0^{-1}v_{n-m}^{(\pm1)}$ to find the nonresonant quantities

$$v_n^{(0)}=\frac{1}{en_0}\sum_m\big(u_{n-m}^{(1)}v_m^{(-1)}+u_{n-m}^{(-1)}v_m^{(1)}\big)$$
$$=\frac{1}{{\rm i}\omega_0}\left[\frac{\partial v^{(1)}}{\partial x}\,v^{(-1)}-\frac{\partial v^{(-1)}}{\partial x}\,v^{(1)}\right]_n,\qquad(3.11)$$

$$u_n^{(0)}+en_{{\rm i},\,n}=-\frac{m_{\rm e}}{4\pi e}\left[\frac{\partial^2}{\partial x^2}\big(v^{(1)}v^{(-1)}\big)\right]_n,\qquad(3.12)$$

$$v_n^{(\pm2)}=\mp\,\frac{k_0}{\omega_0}\sum_m mv_{n-m}^{(\pm1)}v_m^{(\pm1)}=\mp\frac{1}{{\rm i}\omega_0}\left[\frac{\partial v^{(\pm1)}}{\partial x}\,v^{(\pm1)}\right]_n,\qquad(3.13)$$

$$u_n^{(\pm2)}=-\frac{k_0^2nen_0}{\omega_{\rm pe}^2}\sum_s sv_s^{(\pm1)}v_{n-s}^{(\pm1)}=\frac{en_0}{\omega_{\rm pe}^2}\left[\frac{\partial}{\partial x}\left(\frac{\partial v^{(\pm1)}}{\partial x}\,v^{(\pm1)}\right)\right]_n.\qquad(3.14)$$

The equation for resonant quantities then takes on the form

$$\pm\,2{\rm i}\omega_0\left[\frac{\partial u_n^{(\pm1)}}{\partial t}\mp{\rm i}\,\frac{\omega_{\rm pe}^2-\omega_0^2+k_0^2n^2v_{T{\rm e}}^2}{2\omega_0}\,u_n^{(\pm1)}\right.$$
$$\left.\mp\,{\rm i}\,\frac{\omega_0n}{2n_0}\sum_m n_{{\rm i},\,n-m}\,\frac{u_m^{(\pm1)}}{m}\right]$$
$$=k_0^2nen_0\sum_m m\big[v_{n-m}^{(0)}v_m^{(\pm1)}+v_{n-m}^{(\pm1)}v_m^{(0)}\big]$$
$$-\,{\rm i}k_0n(\pm{\rm i}\omega_0)\sum_m\big[(u_{n-m}^{(0)}+v_{{\rm i},\,n-m})v_m^{(\pm1)}+u_{n-m}^{(\pm1)}v_m^{(0)}\big]$$
$$+\,k_0^2nen_0\sum_m mv_{n-m}^{(\mp1)}v_m^{(\pm2)}-{\rm i}k_0n(\pm{\rm i}\omega_0)\sum_m u_{n-m}^{(\pm2)}v_m^{(\mp1)}\,.\qquad(3.15)$$

The right-hand side of Eqn (3.15) defines the so-called electron nonlinearity, which comes to nought in the one-dimensional case, as shown in V E Zakharov's work [11] (see also paper [35]). Specifically, the right-hand side of Eqn (3.15) is equal to $(k_0nen_0/\omega_0)I$, with I satisfying the identity

$$I=-\frac{\partial}{\partial x}\left(v^{(\pm1)}\left[\frac{\partial v^{(1)}}{\partial x}\,v^{(-1)}-\frac{\partial v^{(-1)}}{\partial x}\,v^{(1)}\right]\right)$$
$$\mp\,v^{(\pm1)}\,\frac{\partial^2}{\partial x^2}\big[v^{(1)}v^{(-1)}\big]-\frac{\partial v^{(\pm1)}}{\partial x}\left[\frac{\partial v^{(1)}}{\partial x}\,v^{(-1)}-\frac{\partial v^{(-1)}}{\partial x}\,v^{(1)}\right]$$
$$\pm\,v^{(\mp1)}\,\frac{\partial}{\partial x}\left[\frac{\partial v^{(\pm1)}}{\partial x}\,v^{(\pm1)}\right]\pm v^{(\mp1)}\,\frac{\partial}{\partial x}\left[\frac{\partial v^{(\pm1)}}{\partial x}\,v^{(\pm1)}\right]=0\,.\qquad(3.16)$$

Therefore, we can write out the equation for the resonant density perturbations:

$$\frac{\partial u_n^{(\pm1)}}{\partial t}\mp{\rm i}\,\frac{\omega_{\rm pe}^2-\omega_0^2+k_0^2n^2v_{T{\rm e}}^2}{2\omega_0}\,u_n^{(\pm1)}$$
$$\mp\,\frac{\omega_0}{2n_0}\,n\sum_m\frac{n_{{\rm i},\,n-m}}{m}\,u_m^{(\pm1)}=0\,,\qquad(3.17)$$

or, going over to the electric field strength

$$E_n^{(\pm1)}=\frac{4\pi{\rm i}eu_n^{(\pm1)}}{2k_0n}\,,\qquad(3.18)$$

$$\frac{\partial E_n^{(\pm1)}}{\partial t}\mp{\rm i}\,\frac{\omega_{\rm pe}^2-\omega_0^2+k_0^2n^2v_{T{\rm e}}^2}{2\omega_0}\,E_n^{(\pm1)}$$
$$\mp\,{\rm i}\,\frac{\omega_0}{2n_0}\sum_m n_{{\rm i},\,n-m}E_m^{(\pm1)}=0\,.\qquad(3.19)$$

The ions may be described as large particles whose equation of motion takes the form (2.25), and the density is defined by expression (2.26). The slowly varying component of the electric field may be specified as follows. For slow motions, the following approximation holds true [35]:

$$n_{\rm e}=n_0\exp\left(\frac{e\bar{\phi}-U}{T}\right).\qquad(3.20)$$

Therefore, retaining the first terms in the expansion of the Poisson equation, we obtain

$$\frac{\partial^2}{\partial x^2}\,\bar{\phi}=4\pi e\left(\frac{e\bar{\phi}-U}{T}\,n_0-n_{\rm i}\right).\qquad(3.21)$$

Here, $\bar{\phi}$ and $\bar{E}_n = -\mathrm{i}k_0 n\bar{\phi}_n$ are the potential and strength of the field averaged over fast oscillations. For the HF potential, we have

$$U = \sum_n U_n \exp(\mathrm{i}k_0 nx)\,, \tag{3.22}$$

with

$$U_n = \frac{e^2}{4m\omega_{pe}^2}\sum_m E_{n-m}^{(1)}E_m^{(-1)}\,. \tag{3.23}$$

It is evident that the left-hand side of Eqn (3.21) may be ignored when $k_0^2 n^2 v_{Te}^2/\omega_{pe}^2 = v_{Te}^2/v_\Phi^2 \ll 1$, and then the strength of the field averaged over fast oscillations equals

$$\bar{E}_n = -\mathrm{i}k_0 n\bar{\phi}_n = \frac{-\mathrm{i}k_0 n n_{\mathrm{i},n}T}{en_0} + \frac{-\mathrm{i}k_0 ne}{4m\omega_{pe}^2}\sum_m E_{n-m}^{(1)}E_m^{(-1)}\,. \tag{3.24}$$

The ions may be described hydrodynamically as well. The equations for the slow perturbations of the ion density and velocity take the form

$$\frac{\partial n_{\mathrm{i},n}}{\partial t} + v_{\mathrm{i},n}\mathrm{i}k_0 nn_0 = -\mathrm{i}k_0 n\sum_m n_{\mathrm{i},n-m}v_{\mathrm{i},m}\,, \tag{3.25}$$

$$\frac{\partial v_{\mathrm{i},n}}{\partial t} - \frac{e}{M}\,\bar{E} = -\mathrm{i}k_0\sum_m mv_{\mathrm{i},n-m}v_{\mathrm{i},m}\,. \tag{3.26}$$

We assume the right-hand sides of Eqns (3.25) and (3.26) to be small and ignore them. Then, the density perturbations must obey the equation

$$\frac{\partial^2 n_{\mathrm{i},n}}{\partial t^2} + k_0^2 n^2 c_s^2 n_{\mathrm{i},n} = -\frac{k_0^2 n^2}{16\pi M}\sum_m E_{n-m}^{(1)}E_m^{(-1)}\,, \tag{3.27}$$

where the velocity of sound $c_s = \sqrt{T_e/M}$.

Equations (3.19) and (3.27), which take on the forms

$$\mathrm{i}\,\frac{\partial E}{\partial t} + \frac{v_{Te}^2}{2\omega_{pe}}\frac{\partial^2}{\partial x^2}E - \frac{\omega_{pe}}{2n_0}\,n_\mathrm{i}E = 0\,, \tag{3.28}$$

$$\frac{\partial^2 n_\mathrm{i}}{\partial t^2} - c_s^2\,\frac{\partial^2 n_\mathrm{i}}{\partial x^2} = \frac{1}{16\pi M}\,\frac{\partial^2}{\partial x^2}|E|^2 \tag{3.29}$$

when $\omega_0 = \omega_{pe}$, are known as Zakharov's equations [11] in the one-dimensional case.

As is easily verified, for the upper sign the complex-conjugate Eqn (3.19) assumes the form

$$\frac{\partial (E_n^{(1)})^*}{\partial t} + \mathrm{i}\,\frac{\omega_{pe}^2 - \omega_0^2 + k_0^2 n^2 v_{Te}^2}{2\omega_0}(E_n^{(1)})^* + \mathrm{i}\,\frac{\omega_0}{2n_0}\left[n_{\mathrm{i},n}^*(E_0^{(1)})^* + \sum_{m\neq 0} n_{\mathrm{i},n-m}^*(E_m^{(1)})^*\right] = 0\,. \tag{3.30}$$

At the same time, for negative indices, this equation may be written out (in the summation, the umbral index may be replaced: $m \to -m$) as

$$\frac{\partial E_{-n}^{(-1)}}{\partial t} + \mathrm{i}\,\frac{\omega_{pe}^2 - \omega_0^2 + k_0^2 n^2 v_{Te}^2}{2\omega_0}\,E_{-n}^{(-1)} + \mathrm{i}\,\frac{\omega_0}{2n_0}\left[n_{\mathrm{i},-n}E_0^{(-1)} + \sum_{m\neq 0} n_{\mathrm{i},-n+m}E_{-m}^{(-1)}\right] = 0\,. \tag{3.31}$$

It is easy to see that Eqns (2.26) and (3.31) appear identical at $E_{-n}^{(-1)} = (E_n^{(1)})^*$ and $n_{\mathrm{i},-n} = n_{\mathrm{i},n}^*$. In precisely the same way, it may be verified that similar transformations yield $E_n^{(-1)} = (E_{-n}^{(1)})^*$ and $n_{\mathrm{i},-n} = n_{\mathrm{i},n}^*$. Therefore, ion density perturbations possess symmetry: $n_{\mathrm{i},-n} = n_{\mathrm{i},n}^*$. In this case, to correctly describe the ion cavern it would suffice to use the HF field components $E_n^{(1)}$, $E_{-n}^{(1)}$, and $E_0^{(1)}$, as well as the ion density perturbations $n_{\mathrm{i},n}$, since the remaining quantities are expressed in their terms, i.e., it is possible to abandon using the upper index. Under these conditions, system of Eqns (3.18), (3.27) may be written out in the form

$$\frac{\partial E_n}{\partial t} - \mathrm{i}\,\frac{\omega_{pe}^2 - \omega_0^2 + k_0^2 n^2 v_{Te}^2}{2\omega_0}\,E_n - \mathrm{i}\,\frac{\omega_0}{2n_0}\sum_m n_{\mathrm{i},n-m}E_m = 0\,, \tag{3.32}$$

$$\frac{\partial^2 n_{\mathrm{i},n}}{\partial t^2} + k_0^2 n^2 c_s^2 n_{\mathrm{i},n} = -\frac{k_0^2 n^2}{16\pi M}\sum_m E_{n-m}E_{-m}^*\,. \tag{3.33}$$

Below, we restrict ourselves to the consideration of a so-called supersonic instability mode, whereby $\partial^2 n_{\mathrm{i},n}/n_{\mathrm{i},n}\partial t^2 \gg k_n^2 c_s^2$. When describing ions as particles, advantage can be taken of the equations of motion (2.25) and expression (2.26) for the ion density, where the slowly varying electric field strength is given by

$$\bar{E}_n = -\mathrm{i}k_0 n\bar{\phi}_n = \frac{-\mathrm{i}k_0 nn_{\mathrm{i},n}T}{en_0} + \frac{-\mathrm{i}k_0 ne}{4m\omega_{pe}^2}\sum_m E_{n-m}E_{-m}^*\,. \tag{3.34}$$

For the pump field, which is a high-amplitude long-wavelength Langmuir wave in the case under consideration, we obtain the following equation

$$\frac{\partial E_0}{\partial t} - \mathrm{i}\,\frac{\omega_0}{2n_0}\sum_m n_{\mathrm{i},-m}E_m = 0\,. \tag{3.35}$$

Under these conditions, the systems of equations of the hydrodynamic (3.32), (3.33), (3.35) and hybrid (2.26), (3.32), (3.34), (3.35) models may be written out in the form as follows.

3.1 Hydrodynamic Zakharov's model (supersonic mode) under the conditions $W = |E_0|^2/4\pi \ll n_0 T_e$

In this case, the system of equations takes on the form

$$\begin{gathered}
\frac{\partial E_n}{\partial t} - \mathrm{i}\,\frac{\omega_{pe}^2 - \omega_0^2 + k_0^2 n^2 v_{Te}^2}{2\omega_0}\,E_n + \theta\,\frac{n^6}{n_M^6}\,E_n - \mathrm{i}\,\frac{\omega_0}{2n_0}\left[n_{\mathrm{i},n}E_0 + \sum_{m\neq 0} n_{\mathrm{i},n-m}E_m\right] = 0\,,\\
\frac{\partial^2 n_{\mathrm{i},n}}{\partial t^2} = -\frac{k_0^2 n^2}{16\pi M}\left[E_n E_0^* + E_0 E_{-n}^* + \sum_{m\neq 0,n} E_{n-m}E_{-m}^*\right],\\
\frac{\partial E_0}{\partial t} - \mathrm{i}\,\frac{\omega_0}{2n_0}\sum_m n_{\mathrm{i},-m}E_m = 0\,.
\end{gathered} \tag{3.36}$$

3.2 Hybrid Zakharov's model under the conditions $W = |E_0|^2/4\pi \ll n_0 T_e$

In this case, the system of equations is written out as

$$\frac{\partial E_n}{\partial t} - \mathrm{i}\,\frac{\omega_{pe}^2 - \omega_0^2 + k_0^2 n^2 v_{Te}^2}{2\omega_0}\,E_n + \theta\,\frac{n^6}{n_M^6}\,E_n - \mathrm{i}\,\frac{\omega_0}{2n_0}\left[n_{\mathrm{i},n}E_0 + \sum_{m\neq 0} n_{\mathrm{i},n-m}E_m\right] = 0\,,$$

Table 1. Key parameters of the linear theory for Zakharov's and Silin's models.

Parameter	Zakharov's model	Silin's model
Correction squared to the normalized frequency	$(\delta')_1^2 = \dfrac{(\varDelta')^2}{2} \pm \sqrt{\dfrac{(\varDelta')^4}{4} + A'(\varDelta')}$	
Detuning $\varDelta'$	$(\varDelta')_n = \dfrac{\omega_{pe}^2 + v_{Te}^2 k_0^2 n^2 - \omega_0^2}{2\omega_{pe}^2} \approx \dfrac{v_{Te}^2 k_0^2 n^2}{2\omega_{pe}^2}$	$\varDelta' = \varDelta_0' = \dfrac{\omega_{pe}^2 - \omega_0^2}{2\omega_{pe}^2}$
Coefficient A'	$A' = A'(n) = \dfrac{1}{2}\dfrac{m_e}{M}\dfrac{k_0^2 n^2 v_{Te}^2}{2\omega_{pe}}\dfrac{\lvert E_0\rvert^2}{4\pi n_0 T_e}$	$A' = A'(n) = \dfrac{m_e}{M} J_1^2(a_n)$

$$
\begin{aligned}
\bar{E}_n &= -\mathrm{i}k_0 n \bar{\phi}_n = \frac{-\mathrm{i}k_0 n n_{\mathrm{i},n} T}{e n_0} \\
&\quad + \frac{-\mathrm{i}k_0 n e}{4m\omega_{pe}^2}\left[E_n E_0^* + E_0 E_{-n}^* + \sum_{m\neq 0,\,n} E_{n-m}E_{-m}^*\right], \\
\frac{\mathrm{d}^2 x_s}{\mathrm{d}t^2} &= \frac{e}{M}\sum_n \bar{E}_n \exp(\mathrm{i}k_0 n x_s), \\
n_{\mathrm{i},n} &= n_0 \frac{k_0}{2\pi}\int_{-\pi/k_0}^{\pi/k_0} \exp\big(-\mathrm{i}nk_0 x_s(x_{s0},t)\big)\,\mathrm{d}x_{s0}, \\
\frac{\partial E_0}{\partial t} &- \mathrm{i}\,\frac{\omega_0}{2n_0}\sum_m n_{\mathrm{i},-m}E_m = 0,
\end{aligned}
\tag{3.37}
$$

where the term $\theta(n/n_M)^6 E_n$ in the first equations of systems (3.36) and (3.37) models the damping of HF spectrum modes on electrons, with $n_M = 20$.

For $a_n \ll 1$, the equations of hydrodynamic (2.30) and hybrid (2.31) Silin's models coincide, in view of the representation $J_1(a_n) \approx a_n/2$, $J_0(a_n) \approx 1$, and $J_2(a_n) \approx a_n^2/8$, with the equations derived for the nonisothermal plasma of hydrodynamic (3.36) and hybrid (3.37) Zakharov's models, respectively, correct to the magnitude of detuning and with the inclusion of the substitutions $E_0 \to -\mathrm{i}E_0$ and $E_0^* \to \mathrm{i}E_0^*$.

4. Linear theory

We restrict ourselves to the treatment of the most interesting long-wavelength pump case. From Zakharov's equations (3.36) in the linear case, with the use of representation $\partial E/E\partial t \Rightarrow \mathrm{i}\Omega$, it is possible to obtain the dispersion relation for the nonisothermal case in the supersonic limit $\partial^2 n_{\mathrm{i},n}/n_{\mathrm{i},n}\partial t^2 \gg k_0^2 c_s^2 n^2$:

$$
-\Omega^2(\Omega^2 - \varDelta^2) + \varDelta A = 0, \tag{4.1}
$$

where the detuning $\varDelta = v_{Te}^2 n^2 k_0^2/2\omega_p$ and

$$
A = \frac{1}{2}\frac{m_e}{M}\frac{k_0^2 n^2 v_{Te}^2}{2\omega_{pe}}\frac{|E_0|^2}{4\pi n_0 T_e}\,\omega_{pe}^3.
$$

On the other hand, by linearizing Eqns (2.30), we arrive at precisely the same dispersion relation for the cold plasma case, where, however, $\varDelta = \varDelta_0 = (\omega_{pe}^2 - \omega_0^2)/2\omega_0$ and the quantity $A = J_1^2(a_n)\omega_{pe}^3 m/M$. We note that dispersion relations (4.1), for $a_n \ll 1$ and with the changes $E_0 \to -\mathrm{i}E_0$ and $E_0^* \to \mathrm{i}E_0^*$, coincide in these two cases in deciding on the appropriate choice of the detuning. The positive definiteness of the detuning $\varDelta = v_{Te}^2 n^2 k_0^2/2\omega_{pe}$ in Zakharov's model is evident. As for the detuning $\varDelta = (\omega_{pe}^2 - \omega_0^2)/2\omega_0$ in Silin's model, it was shown in monograph [9] that it is also positively defined and is of order δ, at least in the conditions of long-wavelength Langmuir oscillation excitation by a high-current relativistic electron beam.

Table 1 gives the values of the normalized quantities $\delta' = \Omega/\omega_{pe}$ and $A' = A/\omega_{pe}^3$, which correspond to the two models describing the modulation instability of Langmuir waves.

In Zakharov's model, the correction $\delta' = \Omega/\omega_{pe}$ normalized to the Langmuir frequency should, generally speaking, be written out in the form

$$
(\delta')^2 = \frac{(\varDelta')^2}{2} \pm \sqrt{\frac{(\varDelta')^4}{4} + B(\varDelta')^2}, \tag{4.2}
$$

where

$$
B = \frac{1}{2}\frac{m_e}{M}\frac{|E_0|^2}{4\pi n_0 T_e}. \tag{4.3}
$$

With an increase in $\varDelta'$, the magnitude of $[(\varDelta')^4 + 4B(\varDelta')^2]^{1/2} - (\varDelta')^2$ increases monotonically without a pronounced maximum, and for small $(\varDelta')^2 \ll B$ we therefore have $\Omega^2 \approx -\varDelta'\sqrt{B}$. In this case, $|\Omega^2| < B$ and the instability increment is given by

$$
\operatorname{Im}\Omega = |\Omega| \approx \left(\frac{k_0^2 n^2 v_{Te}^2}{2\omega_{pe}^2}\right)^{1/2}\left(\frac{1}{2}\frac{|E_0|^2}{4\pi n_0 T_e}\frac{m_e}{M}\right)^{1/4}\omega_{pe}. \tag{4.4}
$$

For large $(\varDelta')^2 \gg B$, the quantity $\Omega^2 \approx -B$, and the instability increment in this case is

$$
\operatorname{Im}\Omega = |\Omega| \approx \left(\frac{1}{2}\frac{|E_0|^2}{4\pi n_0 T_e}\frac{m_e}{M}\right)^{1/2}\omega_{pe}. \tag{4.5}
$$

Hence, it follows that the increment increases with perturbation wavenumber to reach its highest value (4.5) for large values of the wavenumber.

In Silin's model, for a detuning magnitude of $(\varDelta')^3 = A'/2$ or, which is the same, $\varDelta' = (m_e/2M)^{1/3} J_1^{2/3}(a_{n_m})$, the relative increment reaches the following values [14]

$$
\delta' = \pm\frac{\mathrm{i}}{\sqrt[3]{2}}(A')^{1/3} = \pm\frac{\mathrm{i}}{\sqrt[3]{2}}\left(\frac{m_e}{M}\right)^{1/3} J_1^{2/3}(a_n). \tag{4.6}
$$

For perturbations with the wavenumber $k_m = k_0 n_m$, for which $a_{n_m} = 1.84$, the magnitude of the Bessel function is largest and the relative increment for such perturbations reaches its highest value

$$
\delta'_{\max} = \pm 0.44\mathrm{i}\left(\frac{m_e}{M}\right)^{1/3}. \tag{4.7}
$$

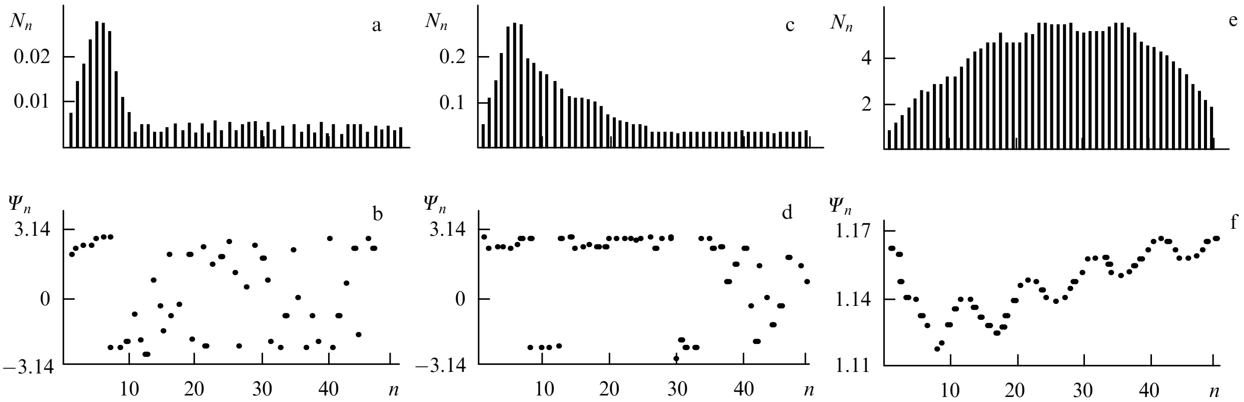

Figure 1. Formation of a wave packet of Langmuir waves upon the development of instability [54]. One can see the mode locking (lower panels) and the spectrum broadening $N_n = N_n \exp(\mathrm{i}\Psi_n)$ (upper panels) for the points in time $\tau = 4$ (a, b), 7 (c, d), and 8 (e, f) [46].

Therefore, the highest increment in Silin's model is exhibited by the wave vectors for which $a_{n_m} = 1.84$. As instability develops, the amplitude of the pump wave lowers and the increment peak shifts to shorter wavelengths.

It is significant that the values of the highest parametric instability increments in Zakharov's model for supersonic perturbations become higher with a decrease in their scale. And, while in Zakharov's model a lowering of the pump field amplitude results in a lowering of the increments throughout the instability domain, in Silin's model this process shifts the increment peak to the short-wavelength domain without decreasing its magnitude (4.7). Therefore, the energy transfer to the short-wavelength part of the spectrum in the two models proceeds largely due to the linear perturbation growth mechanisms.

Furthermore, mention should be made of an explosive amplitude growth of the instability spectrum modes in the supersonic regime of intense Langmuir field decay in a nonisothermal plasma under the conditions $W = |E_0|^2/4\pi \ll n_0 T_e$, which is due to the high values of the increment practically throughout the instability domain. It is precisely this explosive growth of spectrum amplitudes that has been observed in many numerical experiments early in the process.

5. Modulation instability of Langmuir waves in a cold plasma

5.1 Silin's hydrodynamic model

The instability of a powerful long-wavelength (the wavelength is assumed to be infinite) Langmuir wave (pump wave) with the excitation of a short-wavelength Langmuir excitation spectrum may be described by the equations of Silin's hydrodynamic model (2.30) provided that $W = |E_0|^2/4\pi \gg n_0 T_e$.

We utilize the following variables and parameters: $\beta = k_0^2 v_{Te}^2/2\omega_0$, $\Delta_0 = \omega_0(1 - \omega_{pe}^2/\omega_0^2)/2$, $\delta = (m_e/M)^{1/3}\omega_{pe}$, $a = ek_0 E_0/m_e\omega_0^2$, $\tau = \delta t$, $N_n = u_{e,n}^{(1)}/en_0 n$, $M_n = (v_{i,n}/en_0)(\omega_0/\delta)$, $v_{i,n}$ is the Fourier component of the ion density, $E_n = |E_n| \exp(\mathrm{i}\Psi_n)$ is the slowly varying complex amplitude of the electric field strength of plasma electron oscillations with wavenumbers $k_n = nk_0$, where k_0 is the sufficiently small scale selected in the wavenumber space, and $a_n = an$, n are nonzero integers not equal to ± 1, i.e., $n(ek_0 E_0/m_e\omega_0^2) = nk_0 b = a_n$. The density and electric field perturbations are related by the expression $E_n = 4\pi \mathrm{i} e N_n/2k_0 n$; the term $\theta(n/n_M)^6 E_n$ in the first of Eqns (2.30) models the damping of HF spectrum modes on electrons, with $n_M = 20$. The following initial conditions are prescribed: $\beta = 10^{-2}\delta$, $-n_{\max} < n < n_{\max} = 40-100$, $a|_{\tau=0} = 6 \times 10^{-2}$, $\Psi_n|_{\tau=0} = 0$, $M_n|_{\tau=0} = 3 \times 10^{-4}$, and $N_n|_{\tau=0} = 10^{-4}/n$. The characteristics of the instability mode spectrum as functions of time are collected in Fig. 1.

It is significant that the rapid extension of the perturbation spectrum to the short-wavelength domain is largely due to the instability of the pump wave, which follows from a consideration of the linear increment. Indeed, the detuning $\Delta = (\omega_{pe}^2 - \omega_0^2)/2\delta\omega_{pe}$ reaches the value of $(m_e/2M)^{1/3} J_1^{2/3}(a_{n_m})$ for the highest increment of the linear instability normalized to the Langmuir wave frequency [14]:

$$\frac{\delta}{\omega_{pe}} = \frac{\mathrm{i}}{\sqrt[3]{2}} \left(\frac{m_e}{M}\right)^{1/3} J_1^{2/3}(a_n)\,. \tag{5.1}$$

With a lowering of the pump wave amplitude, the increment maximum shifts towards higher wavenumbers without changing its value. Furthermore, the pump wave favors the locking of growing spectrum modes, thereby forming the spatial structure of the cavern (the dimples in the electron and ion plasma densities, which, generally speaking, do not coincide in shape) and the HF filling. By solving the system of Eqns (3.19), one may verify [54] that the energy stored in the short-eavelength part of the Langmuir wave spectrum driven by the pump wave increases, this part of the spectrum rapidly broadening in wavenumber space. The instability results in a shortening of cavern linear dimensions in the configuration space and the formation of relatively steep density gradients whose breaking should generally result in an intense spectrum energy transfer to the plasma electrons. However, there is no way of describing this process in the framework of the model under consideration. The ion density behavior also shows a tendency for a transition to the peaking mode. It is precisely this instability of the numerical computation setup that compelled moving to a description of ions as particles.

5.2 Silin's hybrid model

In Silin's hybrid model, electrons are described hydrodynamically, and ions are treated as large particles. The model equations (2.31) were solved choosing the same varied parameters as with the equations of the hydrodynamic model. In the simulations, we used the relationship $k_0 x_s = 2\pi\xi_s$; the ion-simulating particles, which were taken to be 50 per spectrum mode, were uniformly distributed over the interval $-0.5 < \xi_s < 0.5$. An analysis of the process dynamics showed [48] that this model, too, exhibited the formation of density caverns which were subsequently disrupted. In this case, the disruption was not attended by simulation breakdown. The cause of cavern disruption lay with the field burnup and the inertia of the ion-simulating particles whose number did not exceed 5×10^3 in the numerical experiment; the number of spectrum modes ranged from 40 to 100.

In so doing, the ion cavern collapsed and the ion component passed into the mode of particle trajectory crossing [47, 48]. The energy extracted by the ions turned out to be on the order of $(m_e/m_i)^{1/3}$ fraction of the initial energy of the pump wave [48] (here, m_e and m_i are the electron and ion masses, respectively). Figure 2 shows the behavior of the pump wave for low absorption levels and small initial fluctuations. The bulk of pump field energy goes into the energy of the short-wavelength Langmuir spectrum due to the instability; next, it is possible to observe a partial energy exchange between the spectrum and the pump wave, and the ion cavern collapses for $\tau > 40$, i.e., it passes into the particle trajectory crossing mode.

More recently, the instability development in hybrid models was considered at length in papers [58, 59]. The bulk of attention was on modes with a strong absorption of short-wavelength spectrum energy due to Landau damping, which was phenomenologically introduced. The rate of HF mode damping determined the rate of field burnup in the density caverns, from which the HF field forced out the particles. The bulk of instability energy was initially concentrated in the HF field of the short-wavelength Langmuir spectrum; simultaneously, a low-frequency (LF) perturbation spectrum was formed. Next, the HF spectrum energy was largely transferred to electrons. In this case, the generated density caverns collapsed, the ion trajectories crossed, the ion density perturbations smoothed out, and their scale became longer. The relationship between ion perturbations and the HF field became weaker and the instability saturated. On experiencing several small oscillations, the amplitude of the fundamental wave stabilized at a relatively low level. The bulk of energy was now contained in the perturbations of the plasma electron component. Some small energy fraction on the order of $(m_e/m_i)^{1/3}$ of the initial wave energy was transferred into ion kinetic energy.

5.3 Comparison between Silin's hydrodynamic and hybrid models

The spectrum behavior convinces us that a density cavern forms in the interaction domain, with the cavern dimensions decreasing rapidly [48]. For low energy absorption levels in the system, the instability subsequently transfers to the regime of partial energy exchange between the excited modulation instability spectrum and the pump wave. However, a further decrease in cavern dimensions, i.e., a collapse occurring in the absence of electron pressure in a cold plasma, leads to a simulation breakdown in the hydrodynamic model. On the other hand, the ion inertia, which is naturally included in the hybrid model, permits avoiding such a breakdown. On passing to the trajectory crossing mode, the ions disrupt the cavern and the instability saturates. In this case, it is possible to elucidate the ion

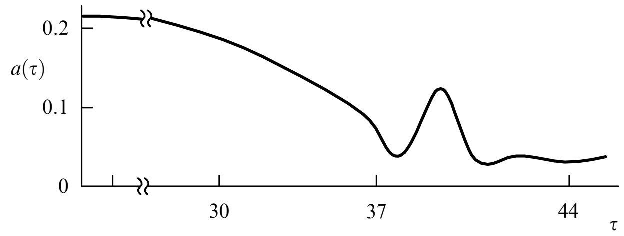

Figure 2. Pump field amplitude $a(\tau)$ as a function of time τ in the hybrid model for a weak absorption of the short-wavelength oscillation energy [40].

velocity distribution. The energy acquired by the ions is on the order of $(m_e/m_i)^{1/3}$ fraction of the initial pump wave energy [48]. Most likely, the energy stored in the short-wavelength Langmuir spectrum is to be largely transferred to the plasma electrons as well. For the electrons, the passage to the trajectory crossing mode (hydrodynamic equations are not applicable in this case for describing electrons) may be hindered by the existence of the ion cavern, which is capable of timing the ejection of fast electrons and ions at the instant of its disruption.

6. Modulation instability of Langmuir waves in a nonisothermal plasma

The instability of a powerful long-wavelength Langmuir wave attended by the excitation of a short-wavelength Langmuir oscillation spectrum may be described by the equations of hydrodynamic (3.36) or hybrid (3.37) Zakharov's models, provided that $W = |E_0|^2/4\pi \ll n_0 T_e$. We discuss the comparison between these models in the numerical experiments described by Clark et al. [49].

In this section, we consider two models: the traditional hydrodynamic Zakharov model (3.36) and the hybrid Zakharov model (3.37). In these systems of equations, the authors of Ref. [49] replaced the last equation for the pump with the equation in the framework of simple weak pump attenuation dynamics. To this end, the researchers put all the parameters equal, the mass ratio was assumed to be $m_e/M = 1/(16 \times 1836)$, the plasma was considered as isothermal, the computational domain $L = 1.8 \times 10^3 \lambda_{de}$, 600 spectral modes were invoked for the hydrodynamic description, and 3000 positions were employed for the hybrid description, i.e., the coordinate plane was divided into this number of segments. As in allied studies (Refs [45, 46]), the authors of Ref. [49] considered the nonself-consistent case of a constant or slowly varying field of an intense Langmuir wave, which was unaffected by the spectrum of short-wavelength perturbations being excited. However, as in the previous case, an important result of this comparison is the revelation of the differences in the process dynamics described by the different models.

First and foremost, Clark et al. [49] noted a significantly faster perturbation growth in the hybrid model, which they attributed to the large magnitudes of ion density perturbations on their selected coordinate grid. Integral characteristics — the HF short-wavelength spectrum energy at the initial stage of the development of modulation instability — turned out to be similar (Fig. 3).

At the initial stage of the developed regime of the process, it was revealed that the relationship between the relative ion density perturbations $\delta n_{i,n}/n_0$ and the short-wavelength field

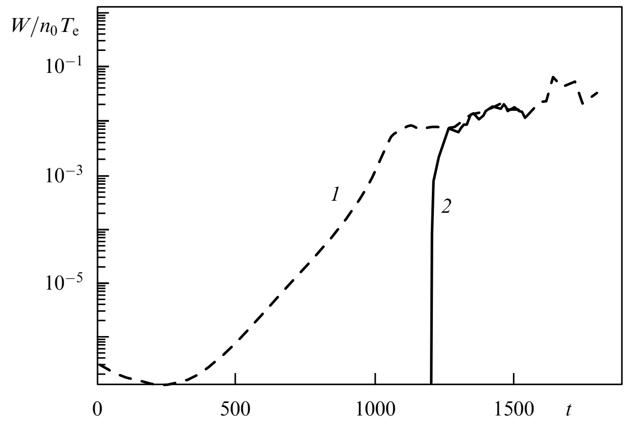

Figure 3. Time (t) dependence of the ratio between the field energy density and the electron thermal energy density for the hydrodynamic (*1*) and hybrid (*2*) Zakharov models [41].

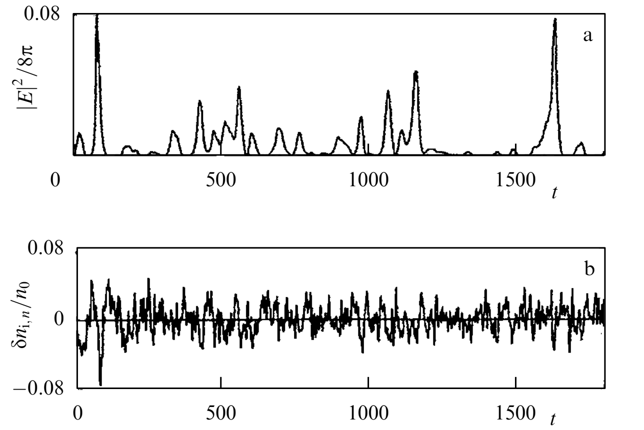

Figure 4. Envelope $|E|^2/8\pi$ of the HF field (a) and relative ion density deviations $\delta n_{i,n}/n_0$ (b) in the hybrid model at the point in time $340\omega_{pe}^{-1}$ [49].

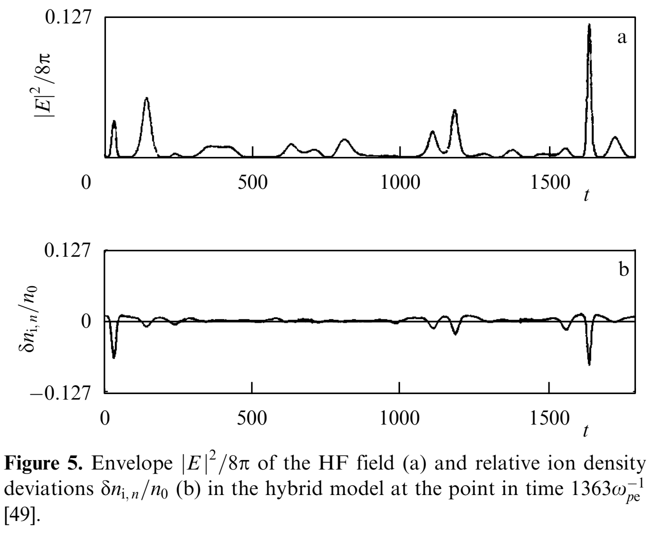

Figure 5. Envelope $|E|^2/8\pi$ of the HF field (a) and relative ion density deviations $\delta n_{i,n}/n_0$ (b) in the hybrid model at the point in time $1363\omega_{pe}^{-1}$ [49].

energy density $|E|^2 = \sum_n |E_n|^2$ held true (Figs 4 and 5):

$$\frac{\delta n_{i,n}}{n_0} \propto \frac{|E|^2}{8}\,. \tag{6.1}$$

Here, for ease of comparison, we chose similar instability regimes which are characterized by about the same peak field amplitudes and density perturbations. First of all, mention should be made of an appreciably greater number of plasma density caverns and significant ion density fluctuations. Accordingly, the number of soliton-like short-wavelength field density perturbations is also greater in the hybrid model. The maximum cavern depths in the hybrid model are always smaller; the characteristic dimensions along the system are similar. Estimates of ion heating under conditions of a constant or slowly varying pump field are hardly of interest, because the authors ignored the effect of the short-wavelength spectrum on the pump.

7. Comparison between Zakharov's and Silin's hybrid models

Below, we compare the development dynamics of the modulation instability of an intense Langmuir wave in two cases of significant interest. In the first case, described by Silin's model, the field energy density is far greater than the thermal energy density of a cold plasma. In the second case, described by Zakharov's model, the field energy density is much lower than the thermal energy density of the non-isothermal plasma, where the ion temperature is well below the plasma temperature.

We emphasize the efficiency of energy transfer to ions and ion perturbations arising from the development of modulation instabilities in nonisothermal and cold plasmas in the framework of the hybrid models.

For each model, we also considered two particular cases: those of light and heavy ions. The parameters employed in these considerations are collected in Table 2. Also of interest is ascertaining how the HF spectrum damping, and accordingly the field burnup in density caverns, affect the energy transfer to the plasma ions.

The number of ion-simulating large particles was selected as follows: $0 < s \leqslant S = 20{,}000$. The large particles were uniformly distributed over the interval $-1/2 < \xi < 1/2$, $\xi = k_0 x/2\pi$, $v_s = \mathrm{d}\xi/\mathrm{d}\tau$, initial conditions for the particles were $\mathrm{d}\xi_s/\mathrm{d}\tau|_{\tau=0} = v_s|_{\tau=0} = 0$, and the number of spectrum modes $-N < n < N$, $N = S/100$. The initial normalized intense-oscillation amplitude $a_0(0) = ek_0E_0(0)/m_e\omega_{pe}^2 = 0.06$. The initial HF mode amplitudes are defined by the expression $e_n|_{\tau=0} = e_{n0} = (2+g)\times 10^{-3}$ in Silin's model, and by the expression $e_n|_{\tau=0} = e_{n0} = (0.5+g)\times 10^{-4}$ in Zakharov's model, where $g \in [0;1]$ is a random number; $ek_0E_n/m_e\omega_{pe}^2 = e_n \exp(\mathrm{i}\psi_n)$, and $\psi_n|_{\tau=0}$ were also randomly distributed over the interval $0-2\pi$. For ion density perturbations n_{ni} and the slowly varying electric field perturbations $\bar{E}_n$, use was made of the also dimensionless representations

$$M_n = M_{nr} + \mathrm{i}M_{ni} = \frac{n_{ni}\omega_{pe}}{n_0\delta} = \frac{\omega_{pe}}{\delta}\int_{-\pi/k_0}^{\pi/k_0} \exp(2\pi n\xi_s)\,\mathrm{d}\xi_{s0}\,,$$

$$\frac{ek_0\bar{E}_n}{m_e\omega_{pe}^2} = E_{nr} + \mathrm{i}E_{ni}\,.$$

The code implementing the mathematical model of the problem was written using the JCUDA technology. The latter provides interaction with the CUDA technology from Java code and furnishes the possibility of performing high-speed parallel computing with a graphics processor.

The instability development in hybrid models (2.31) and (3.37) was considered in papers [58, 59]. The HF mode

Table 2. Parameters of numerical simulations for hybrid models.

Model	Light ions $M/m_e = 2\times10^3$	Heavy ions $m_e/M = 8\times10^{-6}$
Silin's model	$(m_e/M)(\omega_{pe}^2/\delta^2) = 0.43$ $\delta/\omega_0 = 0.44(m_e/M)^{1/3} = 0.034$ $\omega_0/\delta \approx \omega_{pe}/\delta = 29.4$	$(m_e/M)(\omega_{pe}^2/\delta^2) = 0.1$ $\delta/\omega_0 = 0.44(m_e/M)^{1/3} = 0.0088$ $\omega_0/\delta \approx \omega_{pe}/\delta = 113.6$
Zakharov's model	$(m_e/M)(\omega_p^2/\delta^2) = 2n_0T_e/W = 20$ $\omega_0/\delta = 2(n_0T_e/W)^{1/2}(M/m_e)^{1/2} = 282.6$ $\delta/\omega_0 = \delta/\omega_{pe} = 3.5\times10^{-3}$	$(m_e/M)(\omega_p^2/\delta^2) = 2n_0T_e/W = 20$ $\omega_0/\delta = 2(n_0T_e/W)^{1/2}(M/m_e)^{1/2} = 2234.4$ $\delta/\omega_0 = \delta/\omega_{pe} = 4.5\times10^{-4}$

damping rate determined the rate of field burnup in density caverns, from which the HF field forced out the particles. The bulk of instability energy was initially confined in the HF field of the short-wavelength Langmuir spectrum; simultaneously, an LF perturbation spectrum formed. Next, the HF spectrum energy was largely transferred to electrons. In this case, the formed density caverns collapsed, the ion trajectories crossed, the ion density perturbations smoothed out, and their scale became longer. The relationship between ion perturbations and the HF field became weaker and the instability saturated. Having endured several oscillations, the principal wave amplitude was stabilized at a sufficiently low level. The bulk of energy was now contained in the perturbations of the plasma electron component. Some small energy fraction of the initial energy passed to ion kinetic energy. The energy density E_{kin} transferred to the ions was estimated by the expression

$$\frac{E_{kin}}{W_0} \approx 0.27I\,\frac{M}{m_e}\,\frac{\delta^2}{\omega_{pe}^2}\,, \qquad (7.1)$$

where W_0 is the initial energy density of the intense Langmuir wave, $I = \sum_s (d\xi_s/d\tau)^2$ is the appropriately normalized ion energy, and δ is the instability linear increment. The energy fraction of the intense Langmuir wave transferred to the ions was defined by the ratio W_0/n_0T_e in the nonisothermal plasma case (Zakharov's model), and by the ratio $(m/M)^{1/3}$ in the cold plasma case (Silin's model).

Below, we consider in greater detail the integral energy distribution, and the appropriate distribution for LF perturbations in particular [60, 61]. We discuss the peculiarities of the excitation of LF collective ion-acoustic wave motions in a nonisothermal plasma, and of LF oscillations in Silin's model. Special emphasis is laid on the role of HF spectrum absorption responsible for the HF field burnup in density caverns. We will elucidate how this process affects the excitation of the LF spectrum modes and, most important, the form of the ion distribution function and the total energy acquired by the ions.

7.1 Results of numerical simulations

For the parameters $n_M = 20$ and $\Theta = \theta/\delta = 0.05$ determining the character of absorption of an HF energy, Fig. 6 shows the energy of the principal wave, the energy of the small-scale Langmuir spectrum, as well as the energies transferred to plasma electrons and ions normalized to the initial energy of the principal wave.

An analysis of numerical simulation data suggests that the energy of an intense long-wavelength Langmuir wave is at first transferred to the energy of the HF short-wavelength Langmuir spectrum. It is at this stage that plasma density caverns filled by the HF field form. Next, the HF field burns up due to damping on electrons, included phenomenologically in these models (simultaneously transferring its energy to the plasma electrons). Under these conditions, the caverns collapse, LF waves are excited, ion trajectories cross, and the

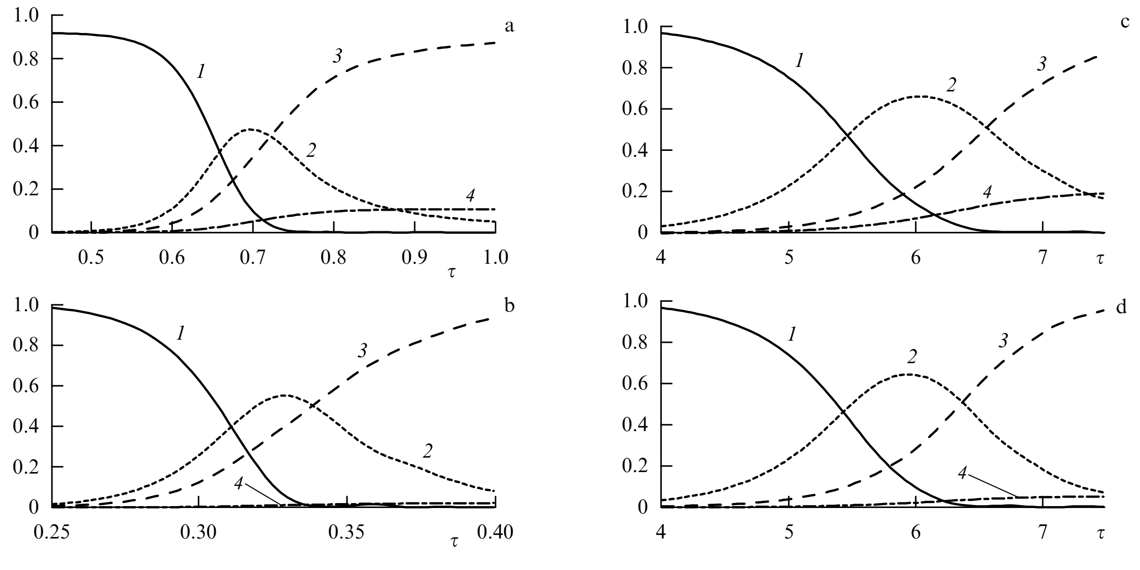

Figure 6. Relative values of the principal wave energy (*1*), the small-scale Langmuir spectrum energy (*2*), the energy transferred to plasma electrons (*3*) and ions (*4*) for Zakharov's (a, b) and Silin's (c, d) models for light (a, c) and heavy (b, d) ions.

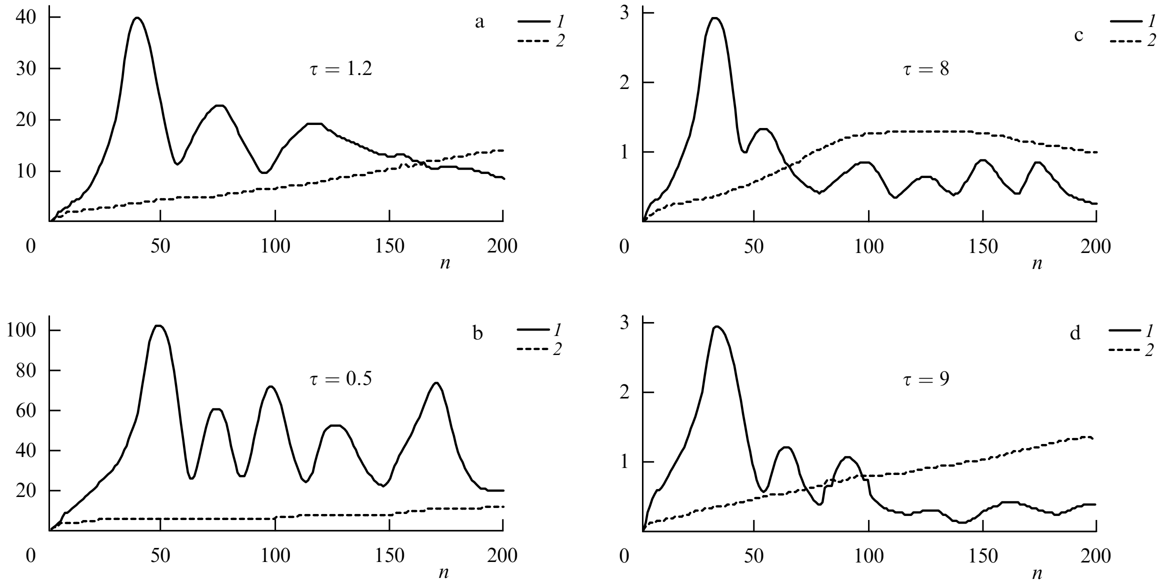

Figure 7. Amplitude of the LF spectral modes and dependence of the frequency on the mode wavenumber for Zakharov's (a, b) and Silin's (c, d) models for light (a, c) and heavy (b, d) ions; *1* — M_n spectrum, and *2* — smoothed average $\partial\Phi_n/\partial\tau$ at the developed instability stage.

energies of the collapsed caverns and the LF spectrum are transferred to ions.

It is possible to determine the root-mean-square ion velocity $\sigma(v_s) = \sqrt{\sum_s v_s^2/S}$ at the end of numerical simulations to obtain $\sigma(v_s) = 0.015$ for light ions, and $\sigma(v_s) = 0.006$ for heavy ones in Zakharov's model. In Silin's model, $\sigma(v_s) = 0.002$ for light ions, and $\sigma(v_s) = 0.0005$ for heavy ones. The total energy of particles in the chosen normalization $I = \sum_s (\mathrm{d}\xi_s/\mathrm{d}\tau)^2$ takes the values 4.689 and 0.808 in Zakharov's models for light and heavy ions, respectively, whereas in Silin's models the respective values are 0.086 and 0.005. The differences in total energy between the models are attributable to the differences in the magnitude of the linear increments, and that between light and heavy ions is due to the choice of ion mass. It is possible to construct a normal distribution proceeding from the root-mean-square velocity, and then the particles that are outside of it (primarily in the so-called tails of the distribution function) possess 13.8% (for the light ions) and 9.2% (for the heavy ions) of the total energy in Zakharov's model. In Silin's model, these figures are appreciably higher: 25.6% (light ions) and 13% (heavy ions). Therefore, a substantially larger fraction of fast particles would be expected in the case of instability of an intense wave in a cold plasma.

Of interest is not only the ion energy distribution, but also the excitation of collective ion oscillations (Fig. 7), and so we determine the frequency of the mode with the wave vector nk_0 for these oscillations:

$$\frac{\mathrm{d}\Phi_n}{\mathrm{d}\tau} = -\left(\frac{\mathrm{d}}{\mathrm{d}\tau}\,\frac{M_{n\mathrm{r}}}{\sqrt{M_{n\mathrm{r}}^2 + M_{n\mathrm{i}}^2}}\right)\left(\frac{M_{n\mathrm{i}}}{\sqrt{M_{n\mathrm{r}}^2 + M_{n\mathrm{i}}^2}}\right)^{-1}, \qquad (7.2)$$

where the phases Φ_n of the LF spectrum modes may be determined from the expression

$$M_n = M_{n\mathrm{r}} + \mathrm{i}M_{n\mathrm{i}} = \sqrt{M_{n\mathrm{r}}^2 + M_{n\mathrm{i}}^2}\,\exp\left(\mathrm{i}\Phi_n\right).$$

Notice that the LF spectrum intensity in the nonisothermal plasma case (Zakharov's model) is rather high in a wide wavenumber range and corresponds to the spectrum of an ion sound after the disruption of density caverns, which was discovered in the numerical experiments [41–44]. By contrast, long-wavelength oscillations prevail in the spectrum for a cold plasma.

In the normalization adopted above, the kinetic ion energy is defined for both models as

$$\frac{1}{2}\int_{-1/2}^{1/2} \mathrm{d}\xi_{s0}\left(\frac{\mathrm{d}\xi_s}{\mathrm{d}\tau}\right)^2, \qquad (7.3)$$

and the collective excitation energies in Zakharov's and Silin's models have the respective forms

$$\begin{gathered}\frac{1}{8\pi^2}\,\frac{m}{M}\,\frac{1}{n_M^2}\,\frac{\delta}{\omega_{\mathrm{pe}}}\sum_n |M_n|^2\,, \\ \frac{1}{8\pi^2}\,\frac{m}{M}\sum_n \frac{1}{n^2}\left[1 - J_0^2(a_n) + \frac{2}{3}\,J_2^2(a_n)\right]|M_n|^2\,,\end{gathered} \qquad (7.4)$$

these oscillations being named ion-acoustic ones in Zakharov's model. Figure 8 plots the variation of the ion energy and the LF field energy with time.

Attention should be drawn to the fact that the LF field energy is much lower than the ion energy in all the cases considered above. The lowering of the field energy with time takes place due to energy transfer to the ions, as well as due to the disruption of plasma density caverns, as pointed out in Ref. [43].

The selected rate of HF field burnup in caverns is defined by the quantity $\Theta = \theta/\delta = 0.05$. It would be instructive to elucidate how the simulated data depend on this parameter. Evidently, not only does the decrease in this parameter slow down the HF field burnup in the caverns, but it also broadens the HF mode spectrum, i.e., increases the fraction of its small-scale components, which deepens the plasma density caverns and raises the kinetic energy of the ions expelled from the caverns. As the HF mode damping becomes weaker, the ion velocity distribution function in the two models approaches progressively closer

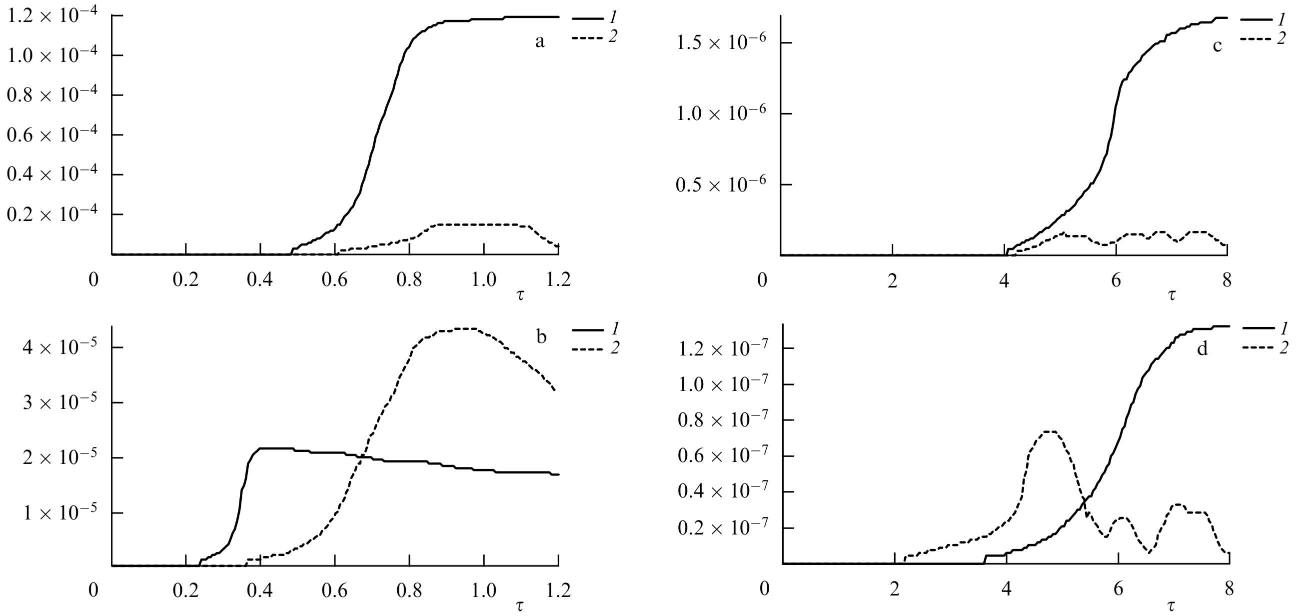

Figure 8. Ion and LF-field energies in Zakharov's (a, b) and Silin's (c, d) models for light (a, c) and heavy (b, d) ions; *1* — kinetic energy, and *2* — oscillation field energy multiplied by 70.

Table 3. Departure of the simulated velocity distribution from the normal distribution.

Absorption level	Hybrid Zakharov's model	Hybrid Silin's model
$\Theta = 0.05$	19.9%	13%
$\Theta = 0.015$	9.9%	13.4%
$\Theta = 0.001$	6.9%	8.8%

to the normal distribution, i.e., the Maxwellian function, which is depicted in Fig. 9.

Table 3 lists the degree of departure of the numerically simulated velocity distribution from the normal velocity distribution of the closest shape (see Fig. 9).

Figure 10 depicts that the highest value of ion-acoustic oscillation energy is hardly changed with a decrease in HF field absorption for nonisothermal plasmas, but the LF spectrum formation speeds up. In cold plasmas, by contrast, the intensity of long-wavelength LF oscillations is appreciably increased with a decrease in HF mode absorption. Subsequently, the LF spectrum is suppressed in transferring its energy to ions.

As would be expected, the energy, which is eventually transferred to the ions, increases with a decrease in HF spectrum absorption in about the same proportion in both nonisothermal and cold plasmas (Fig. 11).

In summary, we note that scales of ion density perturbations shorter than the Debye ion radius $r_{\mathrm{Di}} = v_{T\mathrm{i}}/\omega_{p\mathrm{i}}$ do not make a contribution to the formation of low-frequency electric fields due to the screening effect. In terms of $r_{\mathrm{Di}}k_0/2\pi$, the Debye ion radius may be estimated [50–52] as

$$\frac{r_{\mathrm{Di}}k_0}{2\pi} = R_{\mathrm{Di}} \propto \left\langle \frac{v_{\mathrm{i}}k_0}{2\pi\gamma_L} \right\rangle \frac{\delta}{\omega_{pe}} \left(\frac{M}{m_{\mathrm{e}}}\right)^{1/2} = \langle v_s \rangle \frac{\delta}{\omega_{pe}} \left(\frac{M}{m_{\mathrm{e}}}\right)^{1/2}. \tag{7.5}$$

In the developed instability mode, this quantity gives $R_{\mathrm{Di}} \leqslant 10^{-3}$, and the number of ion density spectral modes does not exceed the quantity $1/R_{\mathrm{Di}}$, which is not at variance with the analysis performed in this work.

8. Conclusions

It was shown that the mechanism of nonlinear Langmuir oscillation absorption occurring when the plasma thermal energy density exceeds the HF field density, which was discovered by V E Zakharov in 1966, also applies to those fields whose energy density far exceeds the thermal plasma energy density. We discussed the similarity of the modulation instability of long-wavelength Langmuir oscillations in hot and cold plasmas, described by Zakharov's and Silin's equations, respectively. The character of perturbation excitation possesses the same symmetry, and the mechanisms of a broad short-wavelength spectrum excitation are also similar. Zakharov's equations for nonisothermal plasmas under conditions when the field energy density is below the thermal energy density of the medium may be derived from Silin's equations for low-temperature plasmas, when the field energy density is substantially higher than the thermal energy density of the medium. Indeed, by lowering the field energy density, it is easy to move from the case analyzed by V P Silin and his colleagues to the case described by Zakharov's equations.

The energy transfer across the spectrum in Zakharov's and Silin's models is not only related to the field restructuring — to the interaction of the modes between themselves — but is largely a consequence of the linear instability. The maximal increments increase upon shortening the perturbation scale in Zakharov's model. The virtually constant increment value in a broad wavenumber range in the supersonic regime gives rise to an explosive growth of plasma density caverns. In Silin's model, the peak increment shifts towards the short-wavelength domain with a decrease in the pump amplitude, which was confirmed by research data on the nonlinear stage of the process. It is also significant that the peak increment in cold plasmas remains invariable on decreasing the pump field amplitude, while the increments in

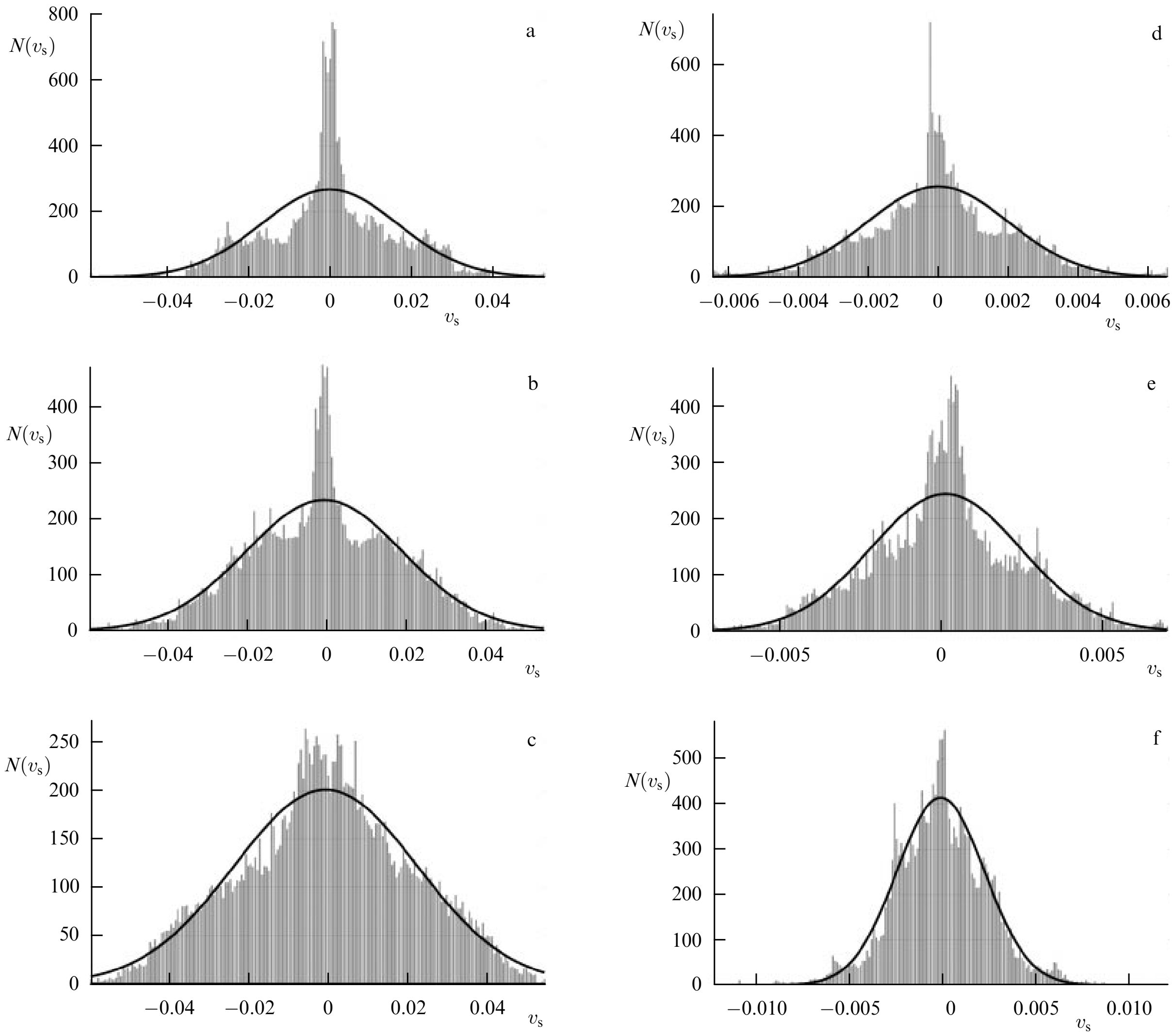

Figure 9. Ion velocity distributions in Zakharov's (a–c) and Silin's (d–f) models for light ions; $\Theta = 0.05$ (a, d), 0.015 (b e), and 0.001 (c, f).

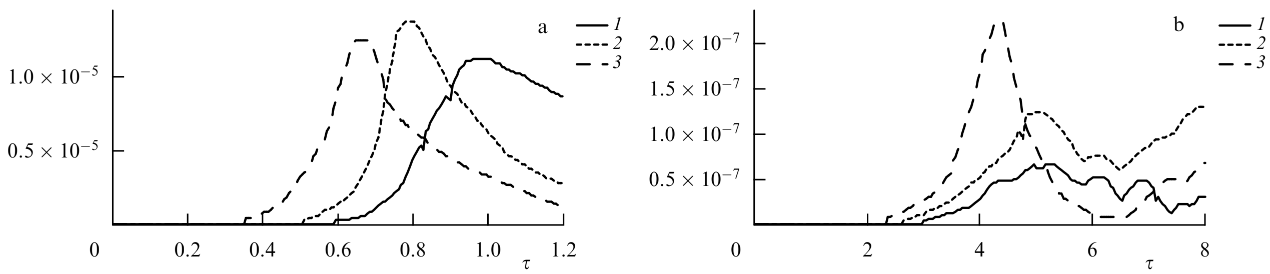

Figure 10. LF spectrum energy as a function of time τ in Zakharov's (a) and Silin's (b) models for light ions; $\Theta = 0.05$ (*1*), 0.015 (*2*), and 0.001 (*3*).

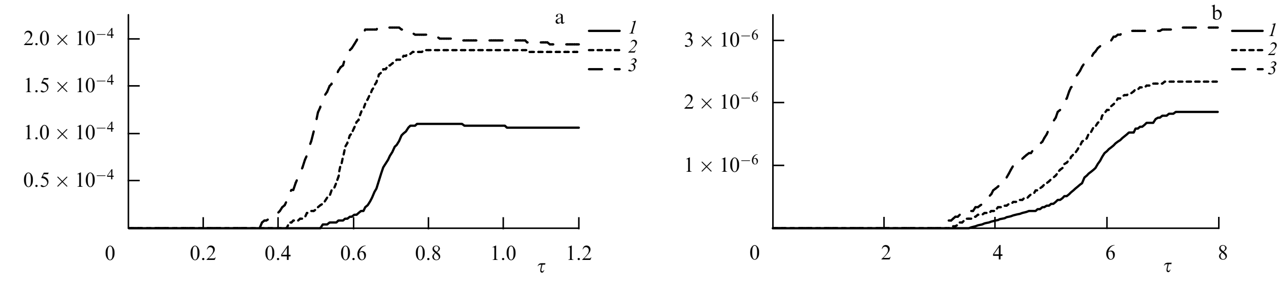

Figure 11. Ion kinetic energy as a function of time τ in Zakharov's (a) and Silin's (b) models for light ions; $\Theta = 0.05$ (*1*), 0.015 (*2*), and 0.001 (*3*).

nonisothermal plasmas under the same conditions become lower throughout the instability domain.

The most significant implication of developing the instability of intense Langmuir waves in plasmas is the transfer of a part of the field energy to the plasma ions and LF oscillations. There is good reason to solve this problem by considering hybrid models, where the electrons are described by quasihydrodynamic equations, and the ions are treated as large particles. The instability processes involving intense long-wavelength Langmuir oscillations turn out to be similar both in hot and in cold plasmas [48, 49].

An analysis of numerical simulation data suggests that the instability of an intense long-wavelength Langmuir wave excites an HF short-wavelength Langmuir spectrum and an LF short-wavelength spectrum. The plasma density caverns filled with the HF field are formed at precisely this stage. Next, the HF field burns up due to damping on electrons included phenomenologically in the models, transferring its energy to plasma electrons. Under these conditions, the caverns collapse, natural LF waves are excited, ion trajectories cross, and the energies of the collapsed caverns and the LF spectrum are transferred to ions. As noted earlier [48], when the field energy density is lower than the thermal energy density of the medium, the fraction of field energy transferred to ions in a nonisothermal plasma is proportional to the ratio of the field energy and the plasma thermal energy. In a cold plasma, the field energy fraction transferred to ions is on the order of the increment-to-frequency ratio or is proportional to the cubic root of the electron-to-ion mass ratio, which is virtually the same thing. In the heavy-ion plasma, the energy transferred to the ion component is appreciably lower than for light ions. In this case, the energy fraction transferred to ions in a cold plasma is inversely proportional to the cubic root of the ion mass. In the hot plasma case, with an increase in ion mass the decrease of the energy fraction transferred to ions becomes more significant [58–60]. The ion energy distribution in Silin's hybrid model exhibits a large fraction of fast particles.

The intensity of the LF spectrum (ion-acoustic waves) in nonisothermal plasmas (Zakharov's model) is of the same order of magnitude in a broad wavenumber range. In a cold plasma (Silin's model), long-wavelength oscillations prevail in the LF spectrum. In this case, the LF field energy turns out to be much lower than the final energy of ions in all the cases considered here. The LF field energy lowers with time due to the energy transfer to the ions.

The lowering of the HF field absorption level corresponds to the moderation of HF field burnup in caverns and broadens the HF mode spectrum, which makes the plasma density caverns deeper and increases the kinetic energy of the ions ejected from the caverns. As the HF mode damping weakens, the ion velocity distribution function in the two models progressively approaches in shape the normal distribution, i.e., the Maxwell function, which permits introducing the ion temperature. The highest value of ion-acoustic oscillation energy is hardly changed with a decrease in HF field absorption in a nonisothermal plasma, but the LF spectrum formation proceeds faster. In a cold plasma, the intensity of precisely the long-wavelength LF oscillations is high, this intensity increasing with a decrease in the level of HF mode absorption. It is significant that the energy eventually transferred to ions increases with a decrease in HF spectrum absorption.

Acknowledgments
The authors express their sincere gratitude to V P Silin and A A Rukhadze for support of this research and their interest in the work, and to E A Kuznetsov for the constructive remarks.

9. Appendix A. Reflection of electromagnetic waves from a bounded plasma

The following problem [62] demonstrates the constructiveness of V P Silin's approach to the description of the parametric instability of an intense field in plasmas. Intense electromagnetic fields acting on the plasma surface give rise to significant oscillations of the electron component. In this case, the electron thermal motion may be ignored and the plasma is treated as cold. The effect of such an electromagnetic field on the surface of a cold plasma was comprehensively analyzed in V P Silin's monograph [16].

Below, we generalize this approach to a self-consistent description of the effect of external electromagnetic radiation normally incident on the plasma boundary, attended by the excitation of a broad spectrum of surface oscillations.

Let an electromagnetic wave with the components $(0, H_y, E_z)$, where $|H_y| = |E_z| = E_0$, be normally incident on a plasma half-space $(x < 0)$ with an unperturbed constant plasma density n_0. The field intensity of the incident wave is assumed to be high enough, and the thermal scatter of the plasma electrons is ignored $(E_0^2 > 4\pi n_0 T_e)$. For the perturbed surface charge density, namely

$$\sigma_\alpha = \lim_{\rho\to 0}\int_{-\rho}^{\rho} n'_\alpha \,\mathrm{d}x\,,$$

where e_α, m_α, and n'_α are the charge, mass, and perturbed charged density of the particles of sort α, we write out the following system of Silin's equations, which he formulated in monograph [16]:

$$\exp\left[\mathrm{i}a_{\alpha n}\sin(\omega_0 t+\varphi)\right]\frac{\partial^2 v_{\alpha,n}}{\partial t^2}+\frac{\omega_\alpha^2}{2}\sum_\beta v_{\beta n}=0\,, \qquad \text{(A.1)}$$

where

$$v_{\alpha,n} = e_\alpha\sigma_{\alpha,n}\exp\left[-\mathrm{i}a_{\alpha,n}\sin(\omega_0 t+\varphi)\right],$$

$$a_{\alpha,n}=\frac{e_\alpha n E_z(k_z=0)}{m_\alpha\omega_0 c}\,,\qquad \omega_\alpha^2=\frac{4\pi e^2 n_0}{m_\alpha}\,,$$

$\omega_0 t+\varphi$ is the phase of the field with $k_z = 0$ in a plasma, and ω_0 is the incident wave frequency. The wavenumber of such perturbations is $k_{zn} = n\omega_0/c$. The solution to Eqn (A.1) will be sought in the form of a series [16]:

$$v_{\alpha,n}=\sum_{s=-\infty}^{+\infty}u_{\alpha,n}^{(s)}\exp(\mathrm{i}s\omega_0 t)\,. \qquad \text{(A.2)}$$

For ion density surface perturbations, one may keep only the first term of the series. The terms in the sum for $v_{e,n}$, proportional to $\exp(\pm\mathrm{i}\omega_0 t)$, exceed the remaining terms of the series, but it is necessary to keep the terms corresponding to the 'zero' and second harmonics. We restrict ourselves to the inclusion of symmetric ion perturbations $u_{i,n}^{(0)} = u_{i,-n}^{(0)}$.

Furthermore, the relations

$$u_{e,n}^{(0)} = u_{e,-n}^{(0)}\,, \quad u_{e,n}^{(\pm 2)} = u_{e,-n}^{(\pm 2)}\,, \quad u_{e,n}^{(\pm 1)} = -u_{e,-n}^{(\pm 1)}\,, \quad (u_{e,n}^{(1)})^* = u_{e,n}^{(-1)}$$

take place.

The self-consistent generalized system of Silin's equations, which takes into account the retroaction of the field of the excited short-wavelength spectrum of surface oscillations on the reflected wave (the parameters of the incident wave, evidently, are invariable) is given in the form

$$\frac{\mathrm{d}u_{e,n}}{\mathrm{d}t} + (\theta_n - \mathrm{i}\Delta_1\omega_0)u_{e,n} = \mathrm{i}\,\frac{\omega_0}{2}\,J_1(a_n)u_{i,n}\exp(\mathrm{i}\varphi)\,, \quad \text{(A.3)}$$

$$\frac{\mathrm{d}^2 u_{i,n}}{\mathrm{d}t^2} = -\omega_0\,\frac{m_e}{M}\,J_1(a_n)\left[u_{e,n}\exp(-\mathrm{i}\varphi) + u_{e,n}^*\exp(\mathrm{i}\varphi)\right], \quad \text{(A.4)}$$

$$D(R - R_0) = \frac{8\pi}{en_0E_0}\sum_n u_{i,n}\left[J_0(a_n)u_{e,n}^*\exp(\mathrm{i}\varphi) - J_2(a_n)u_{e,n}\exp(-\mathrm{i}\varphi)\right], \quad \text{(A.5)}$$

where

$$1 + R = |1 + R|\exp(-\mathrm{i}\varphi) = \frac{a_n\exp(-\mathrm{i}\varphi)}{\beta_0 n}\,,$$

$$\omega_0 = \frac{(1-\Delta_1)\omega_{pe}}{\sqrt{2}}\,, \quad \beta_0 = \frac{2eE_0}{m_e c\omega_0}\,, \quad R_0 = -\frac{D_0^*}{D_0}\,,$$

$$D_0 = \frac{\varepsilon_0}{\kappa_0} + \frac{\mathrm{i}c}{\omega_0}\,, \quad \varepsilon_0 = 1 - \frac{\omega_{pe}^2}{\omega_0^2}\,, \quad \kappa_0^2 = -\frac{\omega_0^2\varepsilon_0}{c^2}\,,$$

$$\Delta_1 = \left(\frac{m_e}{m_i}\right)^{1/3}\Delta\,,$$

R is the amplitude reflection coefficient, $u_{e,n} = u_{e,n}^{(1)}$, and $u_{i,n} = u_{i,n}^{(0)}$.

The terms proportional to $J_0(a_n)$ and $J_2(a_n)$ correspond to the respective contributions from the 'zero' and second harmonics to the nonlinear interaction. From Eqns (A.3)–(A.5) it is possible to derive the relationship

$$1 - |R|^2 = \frac{16\pi}{e\beta_0 n_0 cE_0}\sum_n \frac{1}{n}\left(\frac{\mathrm{d}|u_{e,n}|^2}{\mathrm{d}t} + 2\theta_n|u_{e,n}|^2\right), \quad \text{(A.6)}$$

which embodies the energy conservation law.

To numerically solve Eqns (A.3)–(A.5), we go over to the variables

$$\tau = \left(\frac{m_e}{m_i}\right)^{1/3}\omega_0 t\,, \quad \theta_n = n\theta_0\left(\frac{m_e}{m_i}\right)^{1/3}\omega_0\,,$$

$$u_{e,n} = |u_{e,n}|\exp(\mathrm{i}\varphi_n)\,, \quad N_n = 4\pi\left(\frac{m_e}{m_i}\right)^{1/6}E_0^{-1}|u_{e,n}|\beta_0^{1/2}\,,$$

$$M_n = 4\pi\left(\frac{m_e}{m_i}\right)^{-1/6}E_0^{-1}|u_{i,n}|\beta_0^{1/2}\,.$$

The properties of surface wave damping are such that it becomes stronger with an increase in the oscillation wavenumber [63]. In the course of instability development, the spread in phase φ_n decreases rapidly in a time on the order of a few τ to form the electron and ion surface density domains with rapidly decreasing scale length. This same effect of mode locking leads to a strong interaction of the short-wavelength instability spectrum with the reflected wave and gives rise to significant reflectivity oscillations for a low dissipation in the

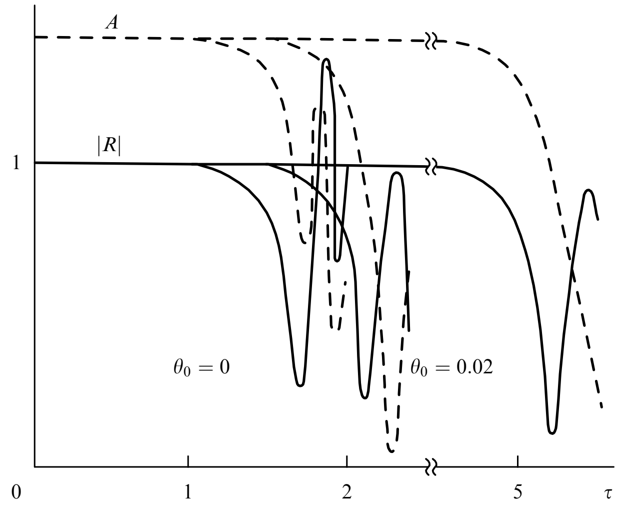

Figure 12. Reflection coefficient R and in-plasma field AE_0 for $\theta_0 = 0$ and $\theta = 0.02$.

interval $R = 0.5-1.3$ (Fig. 12). The inclusion of losses narrows the spatial instability spectrum, lowers the integral level of spectrum energy, and moderates the instability development, with the reflectivity not exceeding unity in its oscillations.

References

1. Fainberg Ya B *Ukr. Fiz. Zh.* **23** 1885 (1978)
2. Rabinovich M S, Rukhadze A A *Sov. J. Plasma Phys.* **2** 715 (1976); *Fiz. Plazmy* **2** 715 (1976)
3. Dawson J M *Phys. Fluids* **7** 981 (1964)
4. Pashinin P P, Prokhorov A M *Sov. Phys. JETP* **33** 883 (1971); *Zh. Eksp. Teor. Fiz.* **60** 1630 (1971)
5. Fainberg Ya B *Sov. J. Plasma Phys.* **11** 803 (1985); *Fiz. Plazmy* **11** 1398 (1985)
6. Kuzelev M V, Rukhadze A A *Elektrodinamika Plotnykh Elektronnykh Puchkov v Plazme* (Electrodynamics of Dense Electron Beams in Plasma) (Moscow: Nauka, 1990)
7. Shapiro V D, Shevchenko V I *Radiophys. Quantum Electron.* **19** 543 (1976); *Izv. Vyssh. Uchebn. Zaved. Radiofiz.* **19** 767 (1976)
8. Kondratenko A N, Kuklin V M *Osnovy Plazmennoi Elektroniki* (Foundations of Plasma Electronics) (Moscow: Energoatomizdat, 1988)
9. Buts V A, Lebedev A N, Kurilko V I *The Theory of Coherent Radiation by Intense Electron Beams* (Berlin: Springer, 2006); Translated from Russian: *Kogerentnoe Izluchenie Intensivnykh Elektronnykh Puchkov* (Moscow: Lebedev Physical Institute of the Russian Academy of Sciences, 2006)
10. Silin V P *Sov. Phys. JETP* **21** 1127 (1965); *Zh. Eksp. Teor. Fiz.* **48** 1679 (1965)
11. Zakharov V E *Sov. Phys. JETP* **24** 455 (1967); *Zh. Eksp. Teor. Fiz.* **51** 688 (1966)
12. Aliev Yu M, Silin V P *Sov. Phys. JETP* **21** 601 (1965); *Zh. Eksp. Teor. Fiz.* **48** 901 (1965)
13. Gorbunov L M, Silin V P *Sov. Phys. JETP* **22** 1347 (1966); *Zh. Eksp. Teor. Fiz.* **49** 1973 (1965)
14. Kruer W L et al. *Phys. Rev. Lett.* **24** 987 (1970)
15. Silin V P *Sov. Phys. Usp.* **15** 742 (1973); *Usp. Fiz. Nauk* **108** 625 (1972)
16. Silin V P *Parametricheskoe Vozdeistvie Izlucheniya Bol'shoi Moshchnosti na Plazmu* (Parametric Effects of Intense Radiation on Plasmas) (Moscow: Nauka, 1973)
17. Zakharov V E *Sov. Phys. JETP* **35** 908 (1972); *Zh. Eksp. Teor. Fiz.* **62** 1745 (1972)
18. Kruer W L *Phys. Fluids* **16** 1548 (1973)

19. Ivanov A A, Nikulin M G *Sov. Phys. JETP* **38** 83 (1974); *Zh. Eksp. Teor. Fiz.* **65** 168 (1973)
20. Kim H C, Stenzel R L, Wong A Y *Phys. Rev. Lett.* **33** 886 (1974)
21. Degtyarev L M, Zakharov V E *JETP Lett.* **21** 4 (1975); *Pis'ma Zh. Eksp. Teor. Fiz.* **21** 9 (1975)
22. Andreev N E, Silin V P, Stenchikov G L *Sov. J. Plasma Phys.* **3** 602 (1977); *Fiz. Plazmy* **3** 1088 (1977)
23. Kovrizhnykh L M *Sov. J. Plasma Phys.* **3** 607 (1977); *Fiz. Plazmy* **3** 1097 (1977)
24. Zakharov V E, L'vov V S, Rubenchik A M *JETP Lett.* **25** 8 (1977); *Pis'ma Zh. Eksp. Teor. Fiz.* **25** 11 (1977)
25. Buchel'nikova N S, Matochkin E P, Preprint No. 79-115 (Novosibirsk: Institute of Nuclear Physics of the USSR Academy of Sciences, 1979)
26. Sagdeev R Z, Shapiro V D, Shevchenko V I *Sov. J. Plasma Phys.* **6** 207 (1980); *Fiz. Plazmy* **6** 377 (1980)
27. Degtyarev L M et al. *Sov. Phys. JETP* **58** 710 (1983); *Zh. Eksp. Teor. Fiz.* **85** 1221 (1983)
28. Wong A Y, Cheung P Y *Phys. Rev. Lett.* **52** 1222 (1984)
29. Cheung P Y, Wong A Y *Phys. Fluids* **28** 1538 (1985)
30. Popel S I, Tsytovich V N, Vladimirov S V *Phys. Plasmas* **1** 2176 (1994)
31. Zakharov V E et al. *Sov. Phys. JETP* **69** 334 (1989); *Zh. Eksp. Teor. Fiz.* **96** 591 (1989)
32. Karfidov D M et al. *Sov. Phys. JETP* **71** 892 (1990); *Zh. Eksp. Teor. Fiz.* **98** 1592 (1990)
33. Vyacheslavov L N et al. *Phys. Plasmas* **2** 2224 (1995)
34. McFarland M D, Wong A Y *Phys. Plasmas* **4** 945 (1997)
35. Kuznetsov E A *Sov. J. Plasma Phys.* **2** 178 (1976); *Fiz. Plazmy* **2** 327 (1976)
36. Zakharov V E *Sov. Phys. Usp.* **31** 672 (1988); *Usp. Fiz. Nauk* **155** 529 (1988)
37. Zakharov V E, Kuznetsov E A *Phys. Usp.* **55** 535 (2012); *Usp. Fiz. Nauk* **182** 569 (2012)
38. Dawson J M, Report No. MATT-152 (Princeton, NJ: Princeton Univ., NJ Plasma Physics Lab., 1962)
39. Shen M-M, Nicholson D R *Phys. Fluids* **30** 1096 (1987)
40. Degtyarev L M et al. *Sov. J. Plasma Phys.* **6** 263 (1980); *Fiz. Plazmy* **6** 485 (1980)
41. Galeev A A et al. *Sov. J. Plasma Phys.* **1** 5 (1975); *Fiz. Plazmy* **1** 10 (1975)
42. Sigov Yu S, Khodyrev Yu V *Sov. Phys. Dokl.* **21** 444 (1976); *Dokl. Akad. Nauk SSSR* **229** 833 (1976)
43. Sigov Yu S, Zakharov V E *J. Physique* **40** (Colloq. C-7) 63 (1979)
44. Robinson P A, de Oliveira G I *Phys. Plasmas* **6** 3057 (1999)
45. Wang J G et al. *Phys. Plasmas* **1** 2531 (1994)
46. Wang J G et al. *Phys. Plasmas* **3** 111 (1996)
47. Kuklin V M, Panchenko I P, Sevidov S M *Radiotekh. Elektron.* **33** 2135 (1988)
48. Chernousenko V V, Kuklin V M, Panchenko I P, in *Integriruemost' i Kineticheskie Uravneniya dlya Solitonov* (Integrability and Kinetic Equations for Solitons) (Managing Eds V G Bar'yakhtar, V E Zakharov, V M Chernousenko) (Kiev: Naukova Dumka, 1990) p. 472
49. Clark K L, Payne G L, Nicholson D R *Phys. Fluids B* **4** 708 (1992)
50. D'yachenko A I et al. *JETP Lett.* **44** 648 (1986); *Pis'ma Zh. Eksp. Teor. Fiz.* **44** 504 (1986)
51. Henri P et al. *Europhys. Lett.* **96** 55004 (2011)
52. Kuklin V M *J. Kharkiv Natl. Univ. Phys. Ser. Nucl. Part. Fields* (1041(2)) 20 (2013)
53. Kuklin V M, in *Proc. Contr. Papers. of Int. Conf. on Plasma Physics, Kiev, April 6 – 12, 1987*, Vol. 4, p. 101
54. Kuklin V M, Sevidov S M *Fiz. Plazmy* **14** 1180 (1988)
55. Koch P, Albritton J *Phys. Rev. Lett.* **32** 1420 (1974)
56. Bulanov S V, Sasorov P V *Sov. J. Plasma Phys.* **12** 29 (1986); *Fiz. Plazmy* **12** 54 (1986)
57. Batanov G M et al. *Sov. J. Plasma Phys.* **12** 317 (1986); *Fiz. Plazmy* **12** 552 (1986)
58. Belkin E V et al. *Vopr. Atom. Nauki Tekh. Plazm. Elektron. Novye Metody Uskoreniya* (4) 260 (2013)
59. Zagorodny A G et al. *Fiz. Osnovy Prib.* **3** (1) 58 (2014)
60. Kirichok A V et al. *Phys. Plasmas* **22** 092118 (2015)
61. Kirichok A V et al., arXiv:1411.3011
62. Kuklin V M, Panchenko I P *JETP Lett.* **43** 302 (1986); *Pis'ma Zh. Eksp. Teor. Fiz.* **43** 237 (1986)
63. Kondratenko A N *Poverkhnostnye i Ob'emnye Volny v Ogranichennoi Plazme* (Surface and Bulk Waves in a Bounded Plasma) (Moscow: Energoatomizdat, 1985)